SSRG International Journal of Civil Engineering
ISSN: 2348-8352/ https://doi.org/10.14445/23488352/IJCE-V12I10P102

Volume 12 Issue 10, 9-36, October 2025

Original Article

Analysis of the Impact of Vertical Geometric Irregularity on the Seismic Stability of Buildings with Viscous Wall Dampers and Viscous Fluid Dissipaters

Franklin Adolfo Lazo Castro[1], Richard Torres Vicente[1], Aldair Edgar Chavez Sedano[1], Manuel Ismael Laurencio Luna[1*]

[1]*Department of Civil Engineering, Continental University, Perú.*

[*]*Corresponding Author : mlaurencio@continental.edu.pe*

Received: 02 August 2025 Revised: 04 September 2025 Accepted: 03 October 2025 Published: 31 October 2025

Abstract - *Peru, located in the Pacific Ring of Fire, faces a high seismic risk, especially along its coastline, where a large-Magnitude Event (Mw 9) with the potential for massive structural impact is predicted. Many mid-rise buildings have Vertical Geometric Irregularities (VGI), characterized by abrupt changes in stiffness or mass between levels, such as setbacks, discontinuities in elements, or structural transitions that amplify drifts, accelerations, and internal stresses during an earthquake. This research analyzes the impact of such irregularity on the seismic stability of 6- to 20-story buildings, incorporating Viscous Wall Dampers (VWD) and Viscous Fluid Dampers (FVD) as passive control systems. Seventeen structural configurations were modeled in ETABS and subjected to a nonlinear time-history analysis using three pairs of scaled real seismic records, in accordance with the requirements of the National Building Code (NBC). The configurations included a base structure without devices and models with one, two, and three control elements located at different levels. Lateral displacements, inter-story drifts, peak accelerations, and shear forces were evaluated. The FVDs demonstrated greater efficiency, achieving reductions of up to 74.42% in displacements, 70.02% in drifts, 65.53% in accelerations, and more than 50% in shear forces, especially in buildings with 12 to 17 floors. VWDs also performed well, with reductions of up to 55.75% in displacements and 51.41% in drifts, improving overall stiffness and torsional response. These results, obtained under a realistic and regulatory approach, offer valuable technical criteria for the preliminary seismic design of structures with vertical irregularity, with potential application in highly seismic urban areas such as Lima, Callao, and other coastal cities in the country.*

Keywords - *Vertical Geometric Irregularity, Viscous Damping Walls, Viscous Fluid Dissipators, Accelerations, Vibration Control.*

1. Introduction

Seismic events represent one of the most significant natural threats to civil structures due to their ability to induce collapse and severe damage, with serious human and economic consequences. Historically, their impact has been devastating, with 2010 being one of the most catastrophic years, registering approximately 227,000 deaths worldwide [1]. More recently, in 2023, a total of 1,781 earthquakes were recorded, 19 of which reached magnitudes between 7.0 and 7.9, confirming the persistence of this hazard [2]. In Latin America, the subduction of the Nazca Plate beneath the South American Plate makes countries such as Mexico, Chile, and Peru highly seismic regions, with a permanent risk of large-magnitude events [3]. In Peru, the Geophysical Institute of Peru (IGP) reports more than 500 perceptible earthquakes annually and warns of the high probability that, in the coming decades, the coastal region will experience a major earthquake [4]. This forecast is based on the nearly 270 years of seismic silence since the great Lima and Callao earthquake of 1746, suggesting the likelihood of a Mw 9.0 event. Peak ground accelerations are expected to reach 500 cm/s² in Lima, between 700 and 900 cm/s² in Callao, and up to 1,100 cm/s² in Ventanilla. The 2007 Pisco earthquake (Mw 7.9), which caused more than 500 deaths, highlighted serious structural deficiencies in many buildings [5, 6]. Combined with rapid urban growth and the aging building stock, this scenario results in high seismic vulnerability. Passive energy dissipation technologies have been developed as practical strategies to mitigate these risks. Among them, Viscous Fluid Dampers (FVDs) reduce displacements and accelerations through velocity-dependent damping mechanisms [7, 8]. In contrast, Viscous Wall Dampers (VWDs) combine stiffness and energy dissipation, controlling torsion, reducing inter-story drifts, and limiting displacements [9-11]. An additional advantage is that they require minimal maintenance, making them particularly suitable for medium- and high-rise buildings.

However, most research has focused on regular structures or on plan-irregular buildings. There is still a lack of systematic comparative studies analyzing the performance of FVDs and VWDs in structures with Vertical Geometric Irregularity (VGI), under scaled real seismic records, and assessing not only global parameters (drifts, displacements, accelerations) but also the redistribution of internal forces in structural frames.

This research performs a systematic numerical evaluation of 6- to 20-story reinforced concrete buildings with VGI, equipped with FVDs and VWDs. Using nonlinear time-history analyses in ETABS, reductions in displacements, drifts, accelerations, and shear forces are quantified, and the redistribution of axial forces, shear, and bending moments is examined.

The novelty lies in identifying the relative efficiency of each system depending on building height and highlighting the complementary role of VWDs as both dissipators and force redistributors.

2. Literature Review

2.1. Vertical Geometric Irregularity and Its Seismic Impact

The Peruvian Technical Standard E.030 – Seismic Design [12] defines Vertical Geometric Irregularity (VGI) as abrupt variations in stiffness, strength, or mass between consecutive stories, manifested through setbacks, reductions in built areas, discontinuities in structural walls, or the presence of soft stories. These configurations disrupt load paths, concentrate forces, and amplify drifts and accelerations, compromising both global stability and the safety of key structural elements. Figure 1 shows examples of buildings in Lima that exhibit VGI [13]. In case (a), a building in Miraflores reduces its built area in the upper levels, creating a setback that concentrates shear demands at the transition story. In case (b), also in Miraflores, a building presents pronounced setbacks and overhangs, interrupting the vertical continuity of columns and walls, which induces torsional irregularities and eccentric load paths. Finally, in case (c), a building in San Borja presents a discontinuous distribution of structural walls, alternating stiff and flexible stories, producing a hinge-like behavior with significant inelastic deformations.

a. Miraflores b. Miraflores c. San Borja

Fig. 1 Buildings with vertical geometric irregularities in Lima, Peru [13]

Figure 2 illustrates collapses associated with VGI in different international seismic events [16–19]. In the 2007 Pisco earthquake (Mw 7.9), many multifamily buildings collapsed due to the absence of confining walls at the ground floor, developing a soft-story mechanism and brittle shear failures in columns. During the 2017 Mexico earthquake (Mw 7.1), several buildings with commercial ground floors collapsed because of their reduced stiffness relative to upper levels, triggering sudden failures. In the 2023 Turkey earthquake (Mw 7.8), more than 6,400 buildings collapsed due to abrupt stiffness transitions and open ground floors, concentrating forces in the first stories and accelerating structural failure mechanisms. These cases confirm that VGI remains one of the leading causes of structural collapse when not adequately addressed in design.

a. Peru 2007 b. Mexico 2017 c. Türkiye 2023

Fig. 2 Collapse of buildings due to vertical geometric irregularity in different earthquakes worldwide [14-16]

2.2. Viscous Wall Dampers (VWD)

The seismic performance of Viscous Wall Dampers (VWDs) has been the subject of several experimental and numerical investigations, demonstrating their potential as both stiffening and dissipative elements in reinforced concrete and steel buildings. In China, reduced-scale shaking table tests (1:4) on a three-story model compared the response of frames with and without VWDs, concluding that these devices increased the structural damping ratio from 3.23% to 6.31% and raised the natural frequency from 1.027 Hz to 3.863 Hz. This dual effect enhanced structural rigidity and introduced additional energy dissipation capacity, resulting in a marked reduction of inter-story drifts under simulated seismic loading [18]. These findings confirm that VWDs act simultaneously as strength and energy dissipation mechanisms, a unique characteristic of other passive devices.

In Japan and the United States, where VWDs have been installed in more than 100 large-scale projects, field reports indicate their consistent ability to reduce inter-story drifts, mitigate floor accelerations, and limit the inelastic demand on structural elements [19]. The fact that their application has expanded to tall buildings in seismic-prone areas demonstrates the confidence in their dual role of stiffness enhancement and damping. In Turkey, optimization-based studies employing metaheuristic algorithms such as Bat and Dragonfly, combined with nonlinear dynamic analyses in ETABS and MATLAB, showed that the strategic placement of VWDs in the lower stories of moment-resisting frames maximizes their effectiveness. This is because lower levels accumulate greater energy demands during seismic excitation, making these locations optimal for dissipation and drift control [20].

Other investigations in Malaysia focused on the interaction between adjacent structures, evaluating the role of VWDs in mitigating seismic pounding. Two ten-story reinforced concrete buildings coupled through VWDs were modeled, and nonlinear dynamic analysis revealed that the devices not only reduced the seismic response of each structure individually but also controlled the transmission of energy between them. However, the efficiency of this strategy was highly sensitive to the damping coefficient assumed in design, emphasizing the need for accurate parameter calibration [21]. In Turkey, large-scale studies on a 30-story reinforced concrete building under a maximum credible earthquake scenario reported that VWDs reduced peak inter-story drifts from above 2% to less than 1.5%, meeting performance targets established by seismic codes [22].

In summary, the literature demonstrates that VWDs are highly effective in reducing global displacements and inter-story drifts while providing additional stiffness and torsional control. Importantly, they also have the potential to redistribute demands along the structural frame, relieving critical elements such as columns from excessive shear or axial loads. This aspect is crucial yet has not been extensively studied, which motivates further investigation in the context of vertically irregular buildings.

2.3. Viscous Fluid Dampers (FVD)

Viscous Fluid Dampers (FVDs) have been widely tested in structures with both regular and irregular configurations, with most studies confirming their remarkable efficiency in dissipating seismic energy. In India, nonlinear time-history analyses conducted on 5-, 10-, and 15-story reinforced concrete buildings demonstrated substantial improvements when FVDs were installed. Reported reductions included up to 91% in inter-story drifts, 90% in the displacement-to-height ratio, and 99% in the shear-to-weight ratio, proving their ability to significantly alleviate seismic demands [23]. These results underline the capacity of FVDs to improve both displacement and force-related response parameters, reinforcing their role as versatile dissipative devices.

Further research in India targeted buildings with vertical irregularities, such as setback and step-back configurations. The inclusion of FVDs in these structures revealed that their efficiency depends not only on their mechanical properties but also on their placement. When positioned at corners and mid-building levels, they produced considerable reductions in displacements and torsional effects, thereby improving overall seismic stability. This strategic placement helped counteract the amplification of demands caused by geometric discontinuities [24-26].

In Bangladesh, the performance of FVDs was analyzed in four plan-irregular building types: C-shaped, L-shaped, I-shaped, and box-shaped. The study found that device location plays a decisive role: in L-shaped buildings, FVDs installed on side walls were more effective in reducing base shear, while in box- and I-shaped structures, corner placement provided superior results. For C-shaped buildings, both strategies proved effective, though with differentiated outcomes depending on whether the target was displacement reduction or base shear control [29].

A comprehensive study in France involving 70 nonlinear dynamic analyses of buildings with plan and vertical irregularities, ranging from 4 to 20 stories, confirmed the effectiveness of FVDs in reducing torsional moments. Their influence was particularly evident in medium- and high-rise buildings, where torsional irregularities are critical and more difficult to control [28].

2.4. Research Gap

Although both viscous wall and fluid dampers have shown significant potential in mitigating seismic demands, previous studies reveal apparent limitations. In the case of VWDs, most research has concentrated on global drift and displacement reduction. At the same time, their role in redistributing internal forces—particularly axial loads, shear, and bending moments in columns and walls—remains underexplored. For FVDs, the evidence consistently highlights their high efficiency in reducing displacements and accelerations, but studies seldom examine their capacity to mitigate localized force concentrations in vertically irregular buildings.

Furthermore, very few investigations have conducted systematic comparative analyses of FVDs and VWDs in structures with vertical geometric irregularities across different building heights. The majority of available research is fragmented, focusing either on regular frames or on plan irregularities, without addressing the combined challenges posed by vertical irregularity and real seismic records scaled to national code requirements.

This research addresses these shortcomings by implementing a unified methodology that evaluates the global efficiency of both systems and, importantly, their influence on the redistribution of internal forces within structural frames. By doing so, it identifies the relative efficiency of each system according to building height and highlights the complementary role they can play in enhancing both global stability and local protection of critical structural elements.

3. Materials and Methods

3.1. Vertical Geometric Irregularity

Vertical geometric irregularity is associated with poor structural performance, as it generates discontinuities such as recesses, height variations, or displacements in structural elements, which cause stress concentrations [29, 30]. According to Standard E.030 [12], this irregularity occurs when, in any direction, the floor plan dimension of a floor exceeds that of an adjacent floor by more than 1.3 times, excluding roofs and basements. Consequently, its presence requires the structure to be reinforced, which increases the design requirements for structural elements and also raises construction costs. Figure 3 illustrates this type of irregularity.

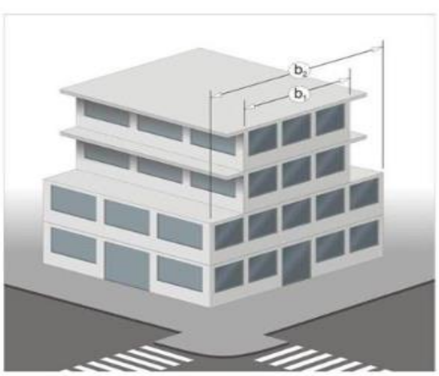

Fig. 3 Vertical Geometric Irregularity [31]

3.2. Seismic Parameters

Seismic parameters were fundamental in evaluating structural response to earthquakes and designing safe buildings [32]. Factors such as zoning, building category, soil type, and structural system were considered, as defined by Standard E.030 [12], which establishes guidelines for earthquake-resistant design. The parameters considered are detailed below.

3.2.1. Zoning

For the study, Lima was considered the area of analysis due to its history of seismic activity in Peru [33]. Figure 4 shows the seismic map of the country, where Lima is located within seismic zone 4, with a value of Z = 0.45.

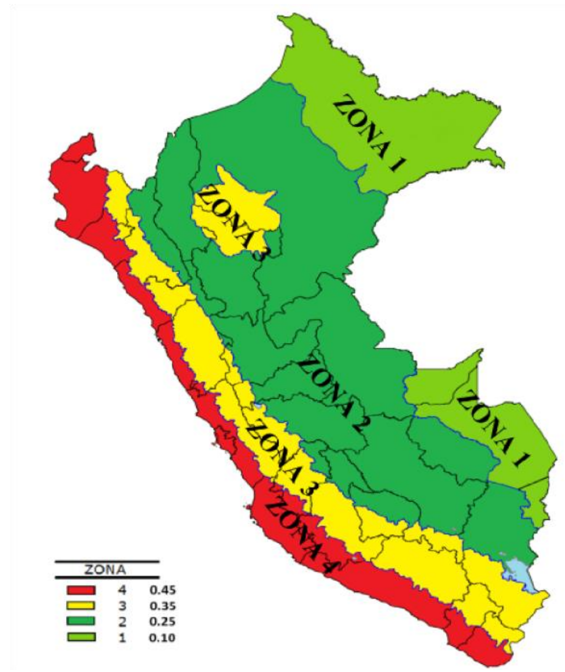

Fig. 4 Seismic zones in Peru [12]

3.2.2. Building Category

In the analysis, typical buildings (U = 1) were used, in accordance with standard E.030 [12]. This type of building includes homes, offices, and hotels, whose failure does not pose additional risks, such as fires or pollutant leaks.

3.2.3. Soil Classification

Soil data from Miraflores and Barranco were used, which correspond to type S1, with a bearing capacity of 4 kg/cm [33], characteristic of hard rock, indicating high resistance and low deformability under seismic loads. In addition, the seismic amplification factor (C) was evaluated in accordance with Article 14 of standard E.030 [14], which establishes that the ratio of the fundamental period factors is Tp(s) = 1 and TL(s) = 1.6, parameters that influence the structural response of the building to seismic events.

3.2.4. Structural System

The structural analysis was based on a dual reinforced concrete system combining moment-resistant frames and structural walls to ensure adequate seismic performance. To reduce seismic forces, the reduction coefficient R was considered, determined in accordance with Article 30 of standard E.030 [12]. This standard establishes that, per section 29.2, time-history analysis must be performed with R = 7, a value corresponding to reinforced concrete structures with dual structural systems.

All these parameters made it possible to calculate the elastic spectrum of pseudo-accelerations, according to Equation (1), thus providing a solid basis for seismic analysis.

$$S_a = \frac{Z.U.C.S}{R}.g \tag{1}$$

Where:

- Z: Zone factor
- U: Use factor
- C: Seismic amplification factor
- S: Soil factor
- R: Seismic force reduction coefficient
- g: Gravity

Figure 5 shows the structural configurations of the 6-, 10-, 15-, and 20-story models, which exhibit vertical geometric irregularity. These models were developed from the data described above and were used to evaluate the effectiveness of viscous walls and viscous fluid devices on the dynamic behavior of the structure.

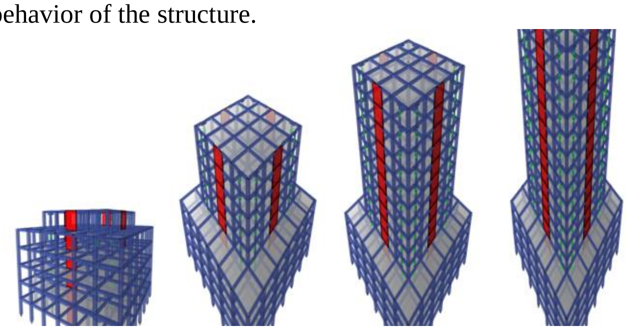

Fig. 5 Structural models with 6, 10, 15, and 20 floors

3.3. Viscous Fluid Damper

The Viscous Fluid Damper is a device used in structures to control vibrations and reduce oscillations during a seismic event or any other dynamic load [32]. Figure 6 shows the Viscous Fluid Damper, where the piston rod (1) moves inside a cylinder (3) filled with a compressible silicone fluid (2). This system dissipates energy through the resistance to movement of the fluid inside the cylinder, providing damping to the structure.

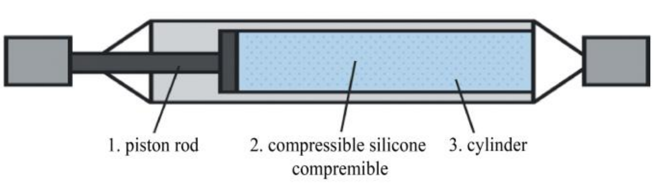

Fig. 6 Viscous fluid damper

To calculate the nonlinear properties of the viscous fluid damper, they are analyzed using FEMA 274, which establishes and calculates the nonlinear damping coefficient from Equation (2).

$$\sum Cj = \frac{\beta h \; x \; 2\pi \; x \; A^{1-\alpha} x \; \omega^{2-\alpha} x \; (\sum_i mi\Phi i^2)}{\lambda(\sum \Phi rj^{1+\alpha} x \; cos^{1+\alpha}\theta j)} \tag{2}$$

Where:

- Subscript j: Dissipator
- Subscript i: Level number
- βh: Viscous damping of the structure
- mi: Mass of level i
- θj: Angle of inclination of the dissipator
- Φi: Modal displacement at level i of the first vibration mode
- Φrj: Relative modal displacement
- A: Amplitude
- ω: Angular frequency
- λ: Lambda parameter

Of the parameters, the angle of inclination of the heat sink (θ_j) and the relative modal displacement (Φ_{rj}) between its ends depend on the location of the device and the lateral displacements at the start and end points where the damper is installed, as illustrated in Figure 7.

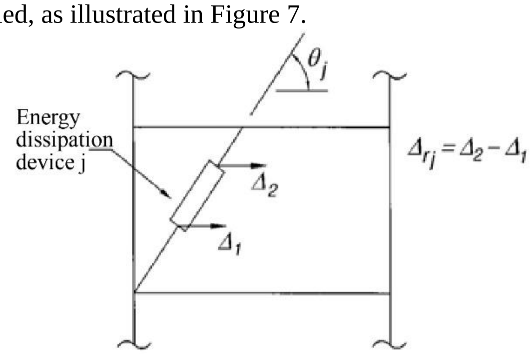

Fig. 7 Energy dissipator

To determine the velocity exponent (α) and the parameter λ, it is necessary to consider whether linear or non-linear viscous dampers will be used, as these values vary according to Table C9-9 of FEMA 274. In general, if a greater damping force is required, α values greater than 1 should be considered. The λ parameter is directly related to the α value and depends on the deformation velocity, as shown in Table 1 below.

In this study, a value of α = 0.5 was adopted, corresponding to moderate nonlinear behavior of the viscous damper. According to Table C9-9 of FEMA 274, this value of α is associated with a parameter λ of 3.5. These parameters allow the dynamic behavior of the damper to be adequately characterized and, based on them, the damping coefficient C is calculated, which represents the device's ability to dissipate energy as a function of the relative deformation velocity.

Table 1. α **and** λ **values**

α	λ
0.25	3.7
0.5	3.5
0.75	3.3
1	3.1
1.25	3
1.5	2.9
1.75	2.8
2	2.7

3.4. Classification of the Poorly Graded Sand Sample with Gravel

Viscous wall dissipators are energy dissipation devices integrated into the walls or partitions of a structure [21]. They are designed to reduce seismic forces by converting the kinetic energy of vibrations into heat through the flow of a viscous fluid within the dissipators [35].

Figure 8 shows a vibration-damping system consisting of an inner plate and an outer plate that encapsulate a viscous or viscoelastic fluid. When a load or vibration is applied, the inner plate moves slightly relative to the outer plate, generating shear in the fluid that dissipates mechanical energy through internal friction, thereby attenuating vibrations, reducing noise transmission, and absorbing impacts in structural, industrial, and transportation applications.

The seismic response of Viscous Wall Dampers (DIS VWDs) was modeled in the ETABS program using nonlinear NLLINK elements, employing the Maxwell exponential damper model [36], as shown in Figure 9. This model represents the behavior of the DIS VWD using a linear spring K in series with a nonlinear viscous damper, characterized by the damping coefficient C and the velocity exponent α, which allows for accurate representation of the system's energy dissipation, especially under nonlinear dynamic loads.

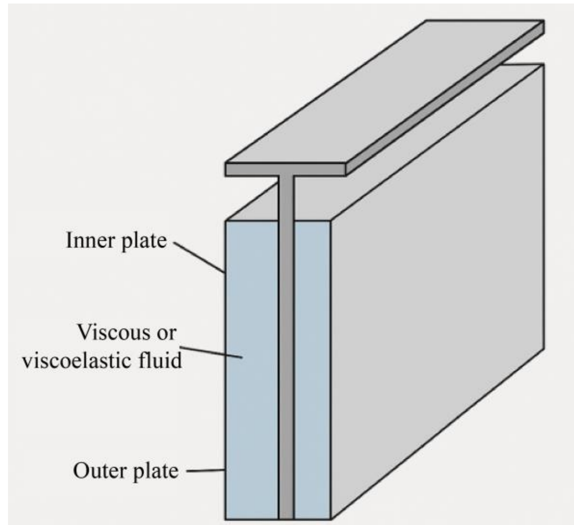

Fig. 8 Viscous Walls

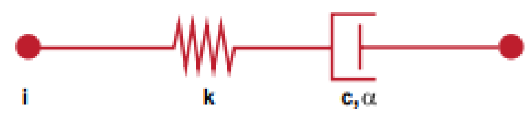

Fig. 9 Maxwell mathematical model [39]

The determination of the model parameters depends mainly on the dimensions of the damper (width and height), as well as its configuration, whether Single Vane or Double Vane. Based on these characteristics, the corresponding values of C, K, and the velocity exponent (α) are assigned, as summarized in Table 2.

Table 2. Maxwell model parameters

DIS VWD	Width (m)	Height (m)	Single Vane		Double Vane		α
			K [ton/m]	C [ton-(sec/m)]	K [ton/m]	C [ton-(sec/m)]	
1.8 x 2.4	1.8	2.4	27500	975	55000	1950	0.5
2.1 x 2.4	2.1	2.4	32000	1225	64000	2450	0.5
2.4 x 2.4	2.4	2.4	35500	1475	71000	2950	0.5

To correctly model a wall with Viscous Wall Dampers (VWD) in ETABS, follow the procedure illustrated in Figure 10. The process begins at the span where the VWD will be installed (between nodes 8 and 10), dividing the beam into three sections so that the central section (between nodes 8 and 10) has a length equal to the width of the damper, which in this case is 7 feet. This central section is then subdivided in half, creating an intermediate node (node 9), resulting in two equal segments. These segments are assigned a Property Modifier ("PM") that increases the inertia (I33) by a factor of 100, thus ensuring that the structural deformation is concentrated in the VWD and not in the beams. Next, two additional nodes (nodes 13 and 14) are added, located halfway between the upper and lower floors, separated horizontally by approximately 15 cm (6 inches). Using highly rigid elements, the center of the upper beam (node 17) is connected to node 13, and the center of the lower beam (node 9) is connected to node 14. Finally, a "2 Joint Link" element is drawn between nodes 13 and 14, which is assigned a "Damper – Exponential" property, entering the stiffness (K), damping (C), and damping exponent (α) values provided by the VWD manufacturer.

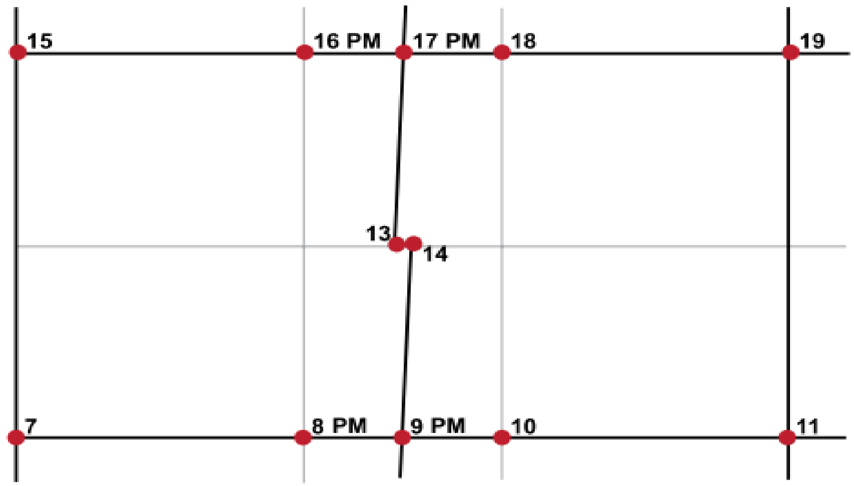

Fig. 10 Example configuration for viscous wall [36]

3.5. Structure Configuration with Viscous Heat Sinks (FVD and VWD)

3.5.1. Configuration with Viscous Fluid Dampers (FVD)

Table 3 shows the structural parameters used for modeling the Viscous Fluid Dampers (FVD) on each floor of the building. A constant floor height of 3.00 m and a metal arm stiffness of 55915.831 tons/m were considered for all floors. Likewise, a constant velocity exponent (α) of 0.50 was maintained, while the nonlinear damping coefficient (ciy) varied according to the floor level, reaching its highest value on the 17th floor with 481.381, which shows a greater demand for energy dissipation at that level. The lowest city values were recorded on the top floors, such as on the 20th floor with 3,500, indicating a lower seismic response requirement at these upper levels. This non-uniform distribution of the damping coefficient reflects the influence of vertical geometric irregularity in the allocation of dissipation devices. Figure 11 shows the structural configuration of the 20-story building, highlighting the strategic location of the viscous fluid dampers. These devices were placed on the diagonals of the structural system, forming part of a double metal bracing system that connects the lower and upper levels, with the aim of maximizing the dissipation of energy induced by seismic loads. Their distribution seeks to act on the areas of most significant relative deformation, thus optimizing the dynamic performance of the building in the event of seismic movements.

Table 3. Properties used for viscous fluid devices

Number of floors	Floor height (m)	Metal arm stiffness (k)	Speed exponent (α)	Nonlinear damping coefficient (ciy)
6.00	3.00	55915.831	0.50	164.931
7.00	3.00	55915.831	0.50	224.800
8.00	3.00	55915.831	0.50	193.054
9.00	3.00	55915.831	0.50	189.581
10.00	3.00	55915.831	0.50	124.071
11.00	3.00	55915.831	0.50	219.336
12.00	3.00	55915.831	0.50	289.094
13.00	3.00	55915.831	0.50	283.891
14.00	3.00	55915.831	0.50	191.994
15.00	3.00	55915.831	0.50	38.851
16.00	3.00	55915.831	0.50	54.002
17.00	3.00	55915.831	0.50	481.381
18.00	3.00	55915.831	0.50	135.842
19.00	3.00	55915.831	0.50	9.957
20.00	3.00	55915.831	0.50	3.500

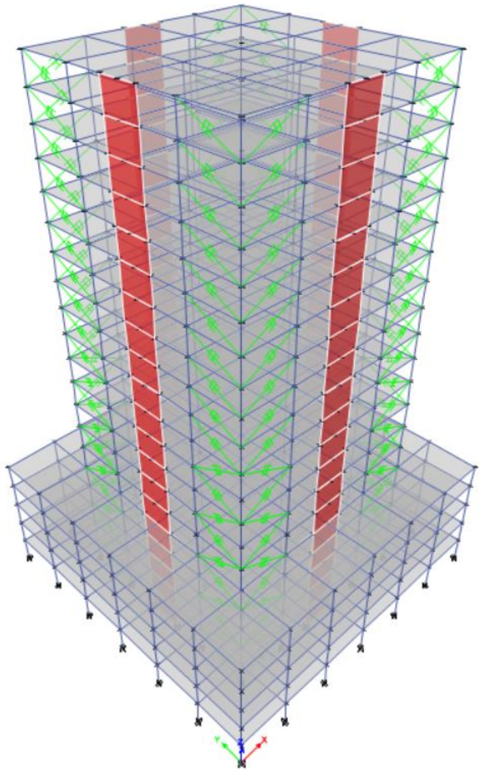

Fig. 10 20-story structure with viscous fluid damper

3.5.2. Configuration with Viscous Wall Dampers (VWD)

On the other hand, Table 4 shows the configuration used for the viscous wall devices, in which specific properties were assigned by level. The floor height was kept constant at 3.00 m, with a velocity exponent (α) of 0.50 for all cases. Unlike the viscous fluid devices, the stiffness of the metal arm (k) varied between floors, registering values of 2804.22, 3263.092, and 3619.993 tons/m, depending on the level.

Likewise, the nonlinear damping coefficient (ciy) ranged from 99.422 to 150.408, with the highest values located on floors 6, 12, and 13, coinciding with greater assigned structural stiffness. This configuration allowed for a more balanced distribution of energy dissipation capacity throughout the height of the building, adapting to the presence of vertical irregularities and different seismic demands per level.

Figure 12 shows a 20-story structure in which viscous walls, represented in green, have been incorporated. These elements are arranged symmetrically as described in section 2.4, which promotes effective control of lateral deformations caused by seismic action. This configuration serves as an apparent visual reference for understanding the integration of these dissipative devices in high-rise buildings, in accordance with the parameters established in Table 4, which details the properties assigned to each level.

Table 4. Properties used for viscous wall devices

Number of floors	Floor height (m)	Metal arm stiffness (k)	Speed exponent (α)	Nonlinear damping coefficient (ciy)
6.00	3.00	3619.993	0.50	150.408
7.00	3.00	3263.092	0.50	124.915
8.00	3.00	2804.22	0.50	99.422
9.00	3.00	2804.22	0.50	99.422
10.00	3.00	2804.22	0.50	99.422
11.00	3.00	3263.092	0.50	124.915
12.00	3.00	3619.993	0.50	150.408
13.00	3.00	3619.993	0.50	150.408
14.00	3.00	2804.22	0.50	99.422
15.00	3.00	2804.22	0.50	99.422
16.00	3.00	2804.22	0.50	99.422
17.00	3.00	3263.092	0.50	124.915
18.00	3.00	2804.22	0.50	99.422
19.00	3.00	2804.22	0.50	99.422
20.00	3.00	2804.22	0.50	99.422

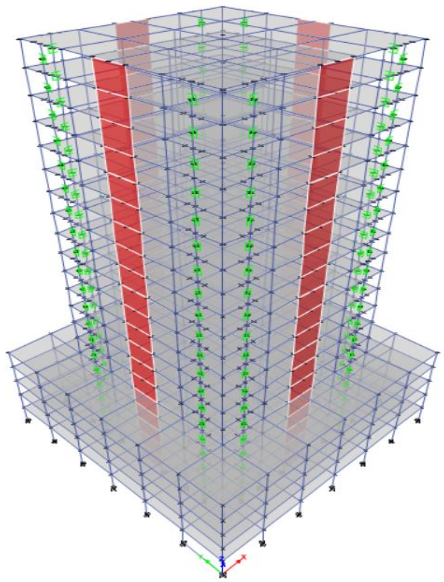

Fig. 11 20-story structure with viscous wall damper

3.5.3. Selected Seismic Records

The reliability of nonlinear time–history analysis critically depends on the quality and representativeness of the ground motion records used. For this reason, the selection of seismic records in this study was carried out under rigorous technical criteria, ensuring that the adopted accelerograms realistically represent the seismic demand at the site and comply with the requirements of the Peruvian Seismic Design Code, NTP E.030 [12]. Three instrumental earthquakes were selected, each representative of the subduction hazard that characterizes the central coast of Peru: the Lima earthquake of October 17, 1966, the Lima earthquake of October 3, 1974, and the Ica earthquake of August 15, 2007. The selection followed five complementary technical criteria:

First is tectonic and regional representativeness since all records correspond to subduction interface events (Nazca–South American plates) with focal mechanisms, frequency content, and durations consistent with the dominant seismicity in Lima. Second, intensity and magnitude compatibility, giving preference to earthquake records with magnitudes close to or above Mw 7, can produce significant seismic demands on medium- and high-rise buildings with vertical geometric irregularity. Third, the availability of orthogonal components (EW and NS) allows the assessment of directional variability of the seismic response and the torsional effects induced by stiffness asymmetries. Fourth, site conditions and source-to-station proximity ensure the use of records from urban stations (Lima and Ica) located at distances consistent with near-field conditions while avoiding signals contaminated by instrumental errors or saturation. Fifth, spectral compatibility with code requirements, achieved by scaling and spectral matching of the records so that the mean 5%-damped response spectra of both horizontal components met or exceeded the target elastic design spectrum of NTP E.030 [12] for seismic zone 4 ($Z = 0.45$) and soil type S1.

The adjustment procedure included baseline correction (integration/de-trending), band-pass filtering to remove spurious low- and high-frequency content while preserving the structural frequency range of interest, and amplitude scaling until compliance with the target spectrum was achieved. Additionally, significant duration (5–95% Arias intensity) and cumulative energy were verified to exclude signals with atypically short durations or non-representative impulsive pulses.

Figure 13 presents the adjusted and scaled records by component: (a) 1966 Lima–EW, (b) 1966 Lima–NS, (c) 1974 Lima–EW, (d) 1974 Lima–NS, (e) 2007 Ica–EW, and (f) 2007 Ica–NS. These adjusted accelerograms were applied simultaneously in their two orthogonal directions during the nonlinear dynamic analyses, ensuring that the seismic input adequately reflected local seismic demand, site amplification effects for S1 soil, and the seismic zone factor defined in E.030 [12].

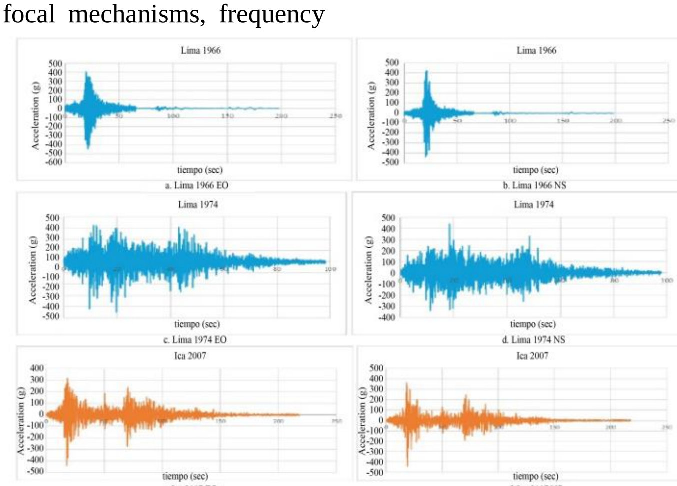

Fig. 12 Amplification of earthquakes

Through this procedure, the selected records not only met the requirements of representativeness and code compliance but also ensured that the structural response obtained from the simulations accurately reflects realistic seismic scenarios for high-rise buildings with vertical geometric irregularities in Lima.

4. Results

4.1. Displacement of Viscous Fluid and Viscous Wall

4.1.1. 6 to 10 Stories

Figure 14 shows the results obtained for maximum displacement in structures incorporating viscous fluid dampers. There is a notable reduction in lateral displacements compared to the structure without devices. For example, in the 6-story structure, the displacement is reduced from 0.1213 m to 0.0954 m, representing a decrease of 21.39%.

In the case of 8 stories, it goes from 0.1704 m to 0.1166 m (31.55% reduction), while in the 10-story structure, the displacement decreases from 0.1991 m to 0.1259 m, achieving an improvement of 36.76%. These results show that viscous fluid dampers are highly effective in controlling seismic displacement, especially in taller buildings.

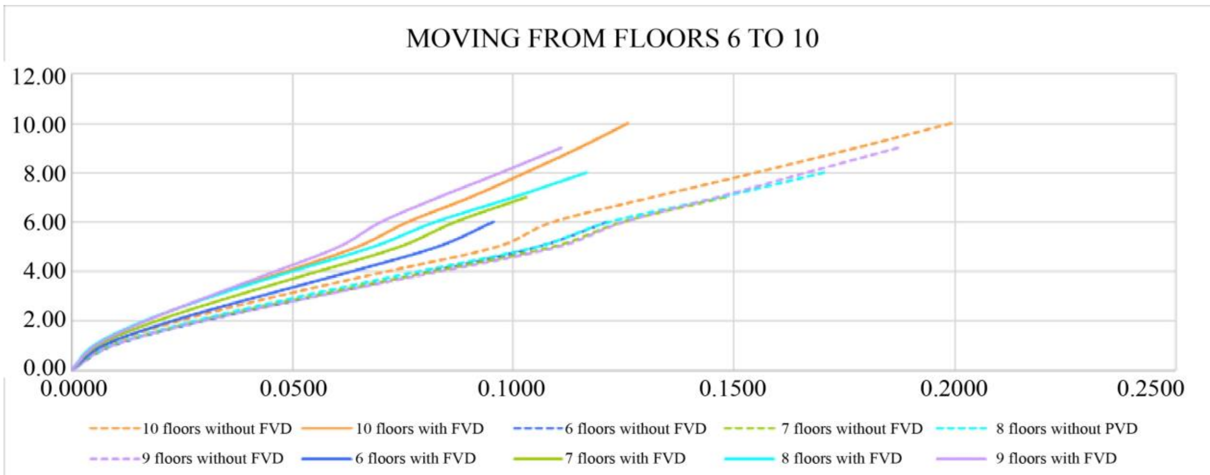

Fig. 13 Displacement of viscous fluid from 6 to 10 floors

Figure 15 shows the effects of incorporating viscous walls in reducing the maximum displacement of the structure. Although their performance is slightly inferior to that of viscous fluid devices, they also achieve a considerable improvement in structural response. For example, in a 6-story structure, the displacement is reduced from 0.1259 m to 0.1033 m, equivalent to a decrease of 17.89%. In the 8-story structure, the displacement goes from 0.1760 m to 0.1417 m, with a reduction of 19.49%, and in the 10-story structure, from 0.2039 m to 0.1377 m, achieving a decrease of 32.45%. These results confirm the usefulness of viscous walls as a passive control system, providing stiffness and energy dissipation capacity in structures subjected to seismic loads.

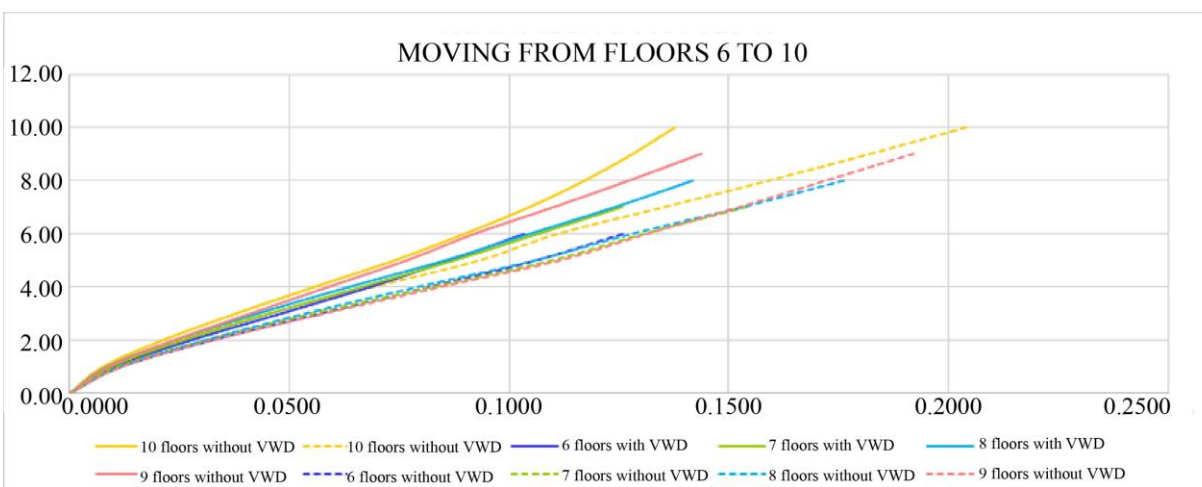

Fig. 14 Displacement of viscous walls from 6 to 10 stories

4.1.2. 11 to 15 Stories

Figure 16 shows the impact of viscous fluid dampers on reducing maximum displacement in structures taller than 10 stories. For example, in the 11-story structure, displacement decreases from 0.1997 m (without a damper) to 0.1061 m with viscous fluid, representing a reduction of 46.89%. In the case of a 13-story structure, the decrease is even more significant: from 0.2543 m to 0.1071 m, with a reduction of 57.89%. However, on the 15th floor, the effect is slightly attenuated, with a decrease of 14.53%, from 0.2496 m to 0.2134 m. These results reflect that, although viscous fluid dampers are generally highly effective in controlling displacement, their performance can vary depending on the structure's height and other structural factors.

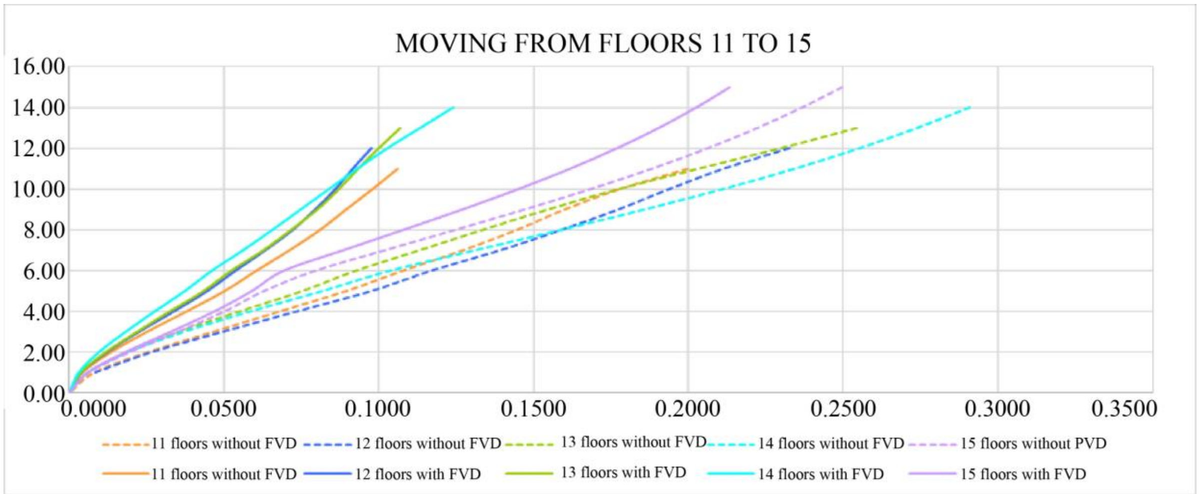

Fig. 15 Displacement of viscous fluid from 11 to 15 floors

Figure 17 analyzes the results obtained with the implementation of viscous walls in structures ranging from 11 to 15 stories. In an 11-story building, displacement is significantly reduced from 0.2108 m to 0.1265 m, i.e., a decrease of 40.01%. This trend continues on intermediate floors, such as on the 13th floor, where displacement decreases from 0.2556 m to 0.1504 m, achieving a reduction of 41.15%. Even in the 15-story structure, viscous walls reduce displacement from 0.2447 m to 0.1530 m, achieving an improvement of 37.49%. These results demonstrate that viscous walls are an effective passive solution, especially useful in medium- to high-rise buildings, contributing to the control of deformations induced by seismic events.

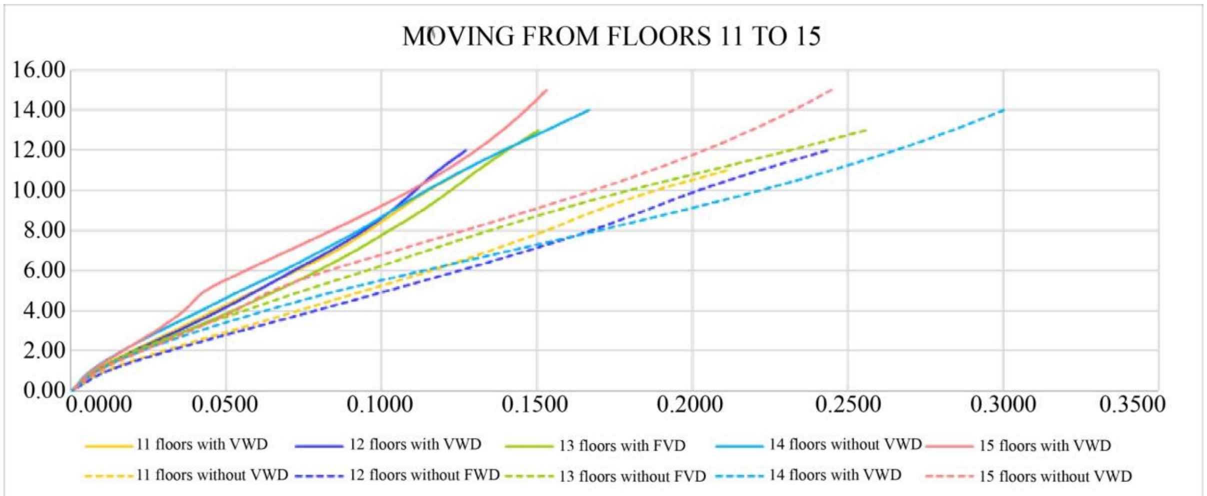

Fig. 16 Displacement of viscous wall from 11 to 15 floors

4.1.3. 16 to 20 Floors

Figure 18 shows significant variations in the effectiveness of viscous fluid dampers as the height of the structure increases. In the case of a 16-story building, there is a moderate reduction in maximum displacement from 0.1870 m to 0.1704 m, representing a decrease of 8.88%. However, in a 17-story building, the performance improves significantly, from 0.3041 m to 0.0778 m, representing a remarkable reduction of 74.42%. In contrast, in a 20-story structure, there is a slight deterioration, where the displacement increases slightly from 0.1663 m to 0.1667 m with the use of viscous fluid, which translates into a negative variation of -0.22%. These results indicate that the effectiveness of fluid dampers may not be linear with height and that their optimal performance could depend on the specific structural configuration of each building.

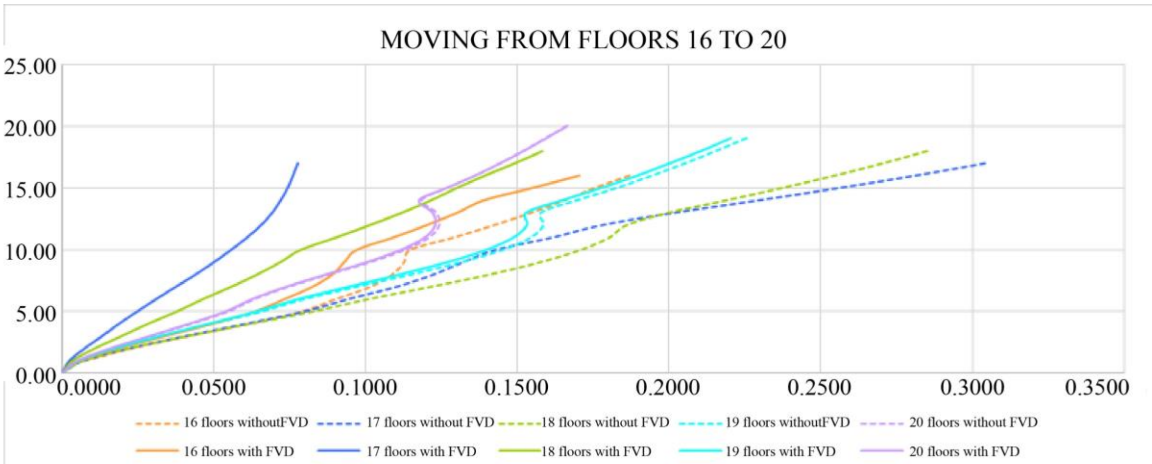

Fig. 17 Displacement of viscous fluid from 16 to 20 floors

In Figure 19, the results obtained with the inclusion of viscous walls also show variable behavior depending on the height of the building. For a 16-story structure, the displacement is reduced from 0.2046 m to 0.1506 m, achieving an improvement of 26.39%. In the case of 17 stories, the effect is more noticeable, decreasing from 0.3133 m to 0.1386 m, with a significant reduction of 55.75%. However, in the 20-story building, the displacement increases slightly from 0.1648 m to 0.1761 m, representing a negative reduction of -6.90%. These results suggest that, although viscous walls can be effective in specific configurations, their performance can also decrease in very tall structures if their location and quantity are not optimized.

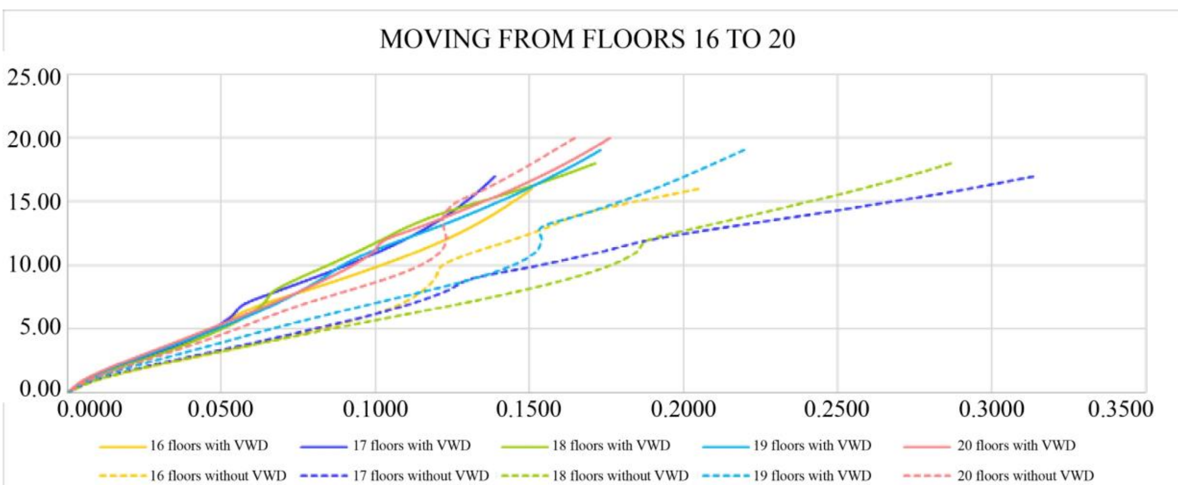

Fig. 18 Displacement of viscous wall from 16 to 20 floors

4.2. Viscous Fluid Drift and Viscous Wall

4.2.1. 6 to 10 stories

Figure 20 shows the results of controlling maximum drifts using viscous fluid dampers. In a 6-story structure, drift is reduced from 0.0087 to 0.0069, representing an improvement of 20.94%. This effect is intensified in taller buildings, such as the 8-story building, where drift decreases from 0.0094 to 0.0062, achieving a reduction of 33.96%. However, in 10-story structures, although the reduction is still significant, it drops to 23.39%, from 0.0091 to 0.0070. These results indicate that viscous fluid dampers consistently contribute to limiting relative lateral deformation between floors, being especially effective in buildings of intermediate height.

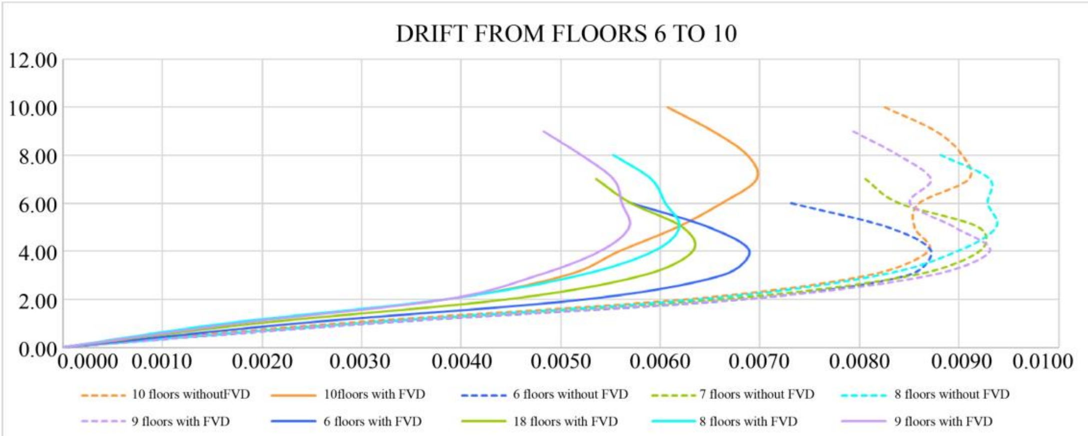

Fig. 19 Viscous fluid drift from 6 to 10 floors

As shown in Figure 21, a considerable reduction in maximum drifts is also achieved regarding the implementation of viscous walls. In a 6-story structure, the drift is reduced from 0.0087 to 0.0071, with an improvement of 18.41%. For 8 stories, the effect is even more pronounced, reducing from 0.0094 to 0.0073, which is equivalent to a decrease of 21.82%. In the case of a 10-story building, viscous walls achieve a reduction of 25.49%, from 0.0091 to 0.0068. These results demonstrate that viscous walls provide a progressive and solid improvement in drift control as the height of the building increases, making them an efficient option for improving structural performance under seismic loads.

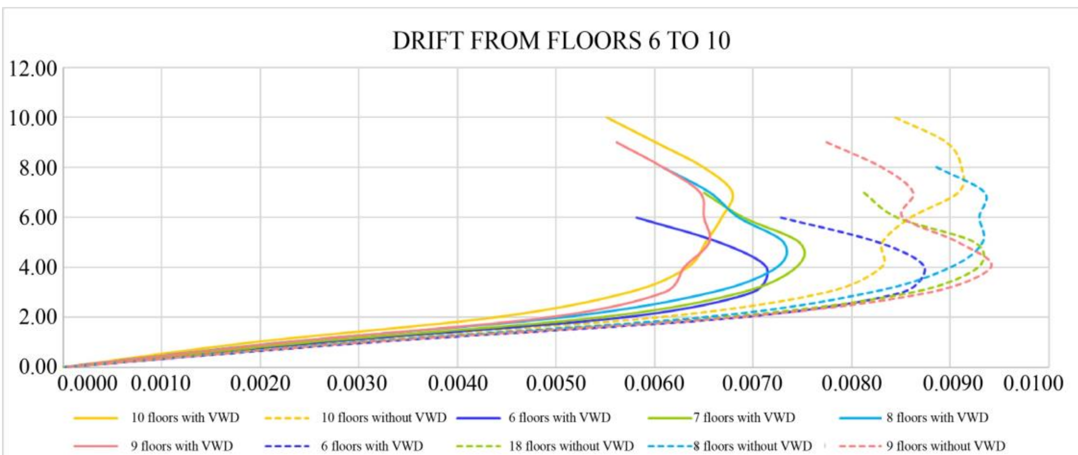

Fig. 20 Viscous fluid drift from 6 to 10 floors

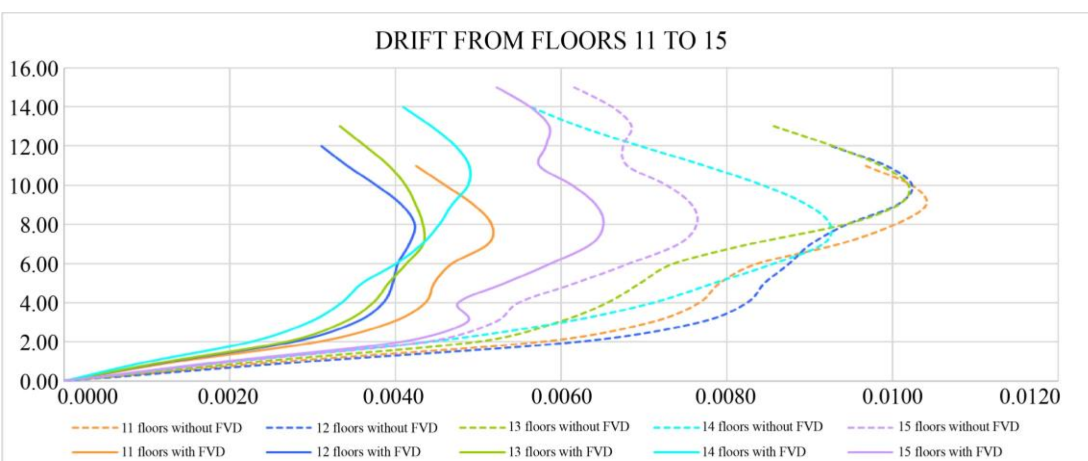

Fig. 21 Viscous fluid drift from 11 to 15 floors

4.2.2. 11 to 15 Stories

Figure 22 shows the positive impact of using viscous fluid dampers in reducing maximum drifts in medium-height structures. For example, in an 11-story structure, the drift decreases from 0.0104 to 0.0052, representing a remarkable reduction of 50.37%. In the case of a 13-story building, a similar behavior is observed, with a reduction of 57.43%, from 0.0102 to 0.0043. For 15 stories, although the decrease is comparatively minor, a 14.68% improvement is achieved, with the drift decreasing from 0.0076 to 0.0065. These results reflect that the viscous fluid system is particularly effective at intermediate heights, contributing significantly to limiting inter-story distortion in the event of seismic events.

Figure 23 shows that viscous walls are also effective in controlling maximum drifts, particularly in taller structures. In an 11-story building, the drift is reduced from 0.0104 to 0.0065, an improvement of 37.91%. For 13 stories, the decrease is 38.66%, falling from 0.0102 to 0.0061.

Finally, in a 15-story structure, the reduction reaches 24.02%, from 0.0076 to 0.0056. These values indicate that viscous walls allow for a considerable reduction in relative lateral deformation, making them a viable and effective technical solution for improving structural performance in earthquakes, especially in buildings over 10 stories tall.

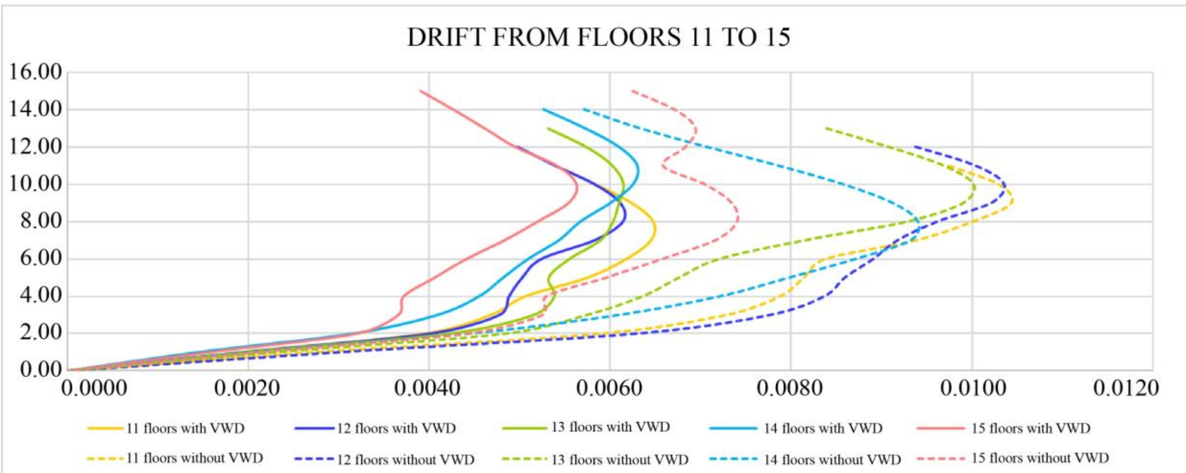

Fig. 22 Viscous wall drift from 11 to 15 stories

4.2.3. 16 to 20 Stories

Figure 24 shows how viscous fluid dampers continue to be effective in reducing maximum drifts in tall structures, although with variations depending on the number of floors. In a 16-story building, the drift is reduced from 0.0079 to 0.0063, achieving an improvement of 20.32%. This effect is intensified in 17-story structures, where the reduction reaches 70.02%, going from 0.0094 to 0.0028. However, for a 20-story building, the effect becomes almost null, with only a 1.87% improvement, dropping from 0.0085 to 0.0084. This suggests that the efficiency of the viscous fluid system may decrease in very tall buildings, possibly due to limitations in the distribution or design of the dissipation system.

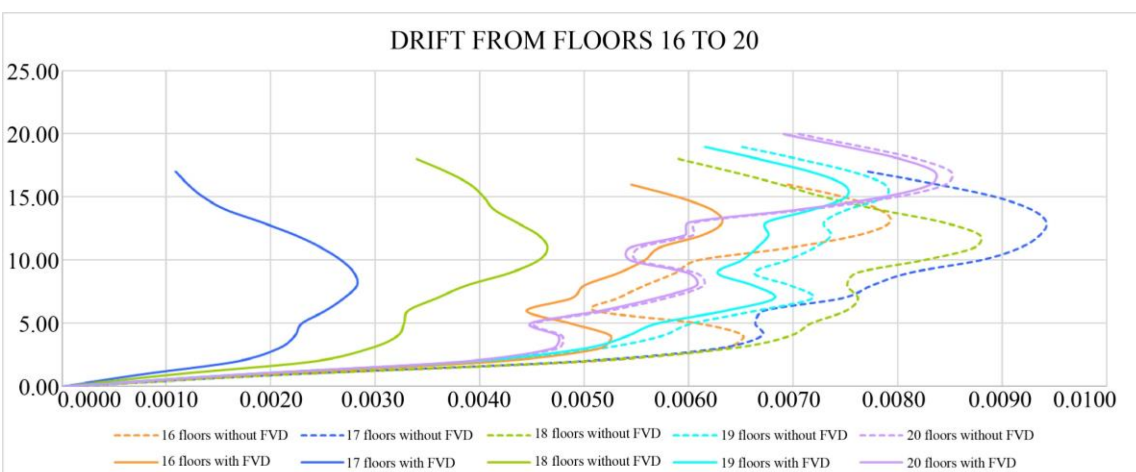

Fig. 23 Viscous fluid drift from 16 to 20 floors.

Figure 25 shows that viscous walls maintain a considerably stable performance in reducing maximum drifts, even in tall structures. In the case of a 16-story building, there is a 37.98% improvement, with drift reduced from 0.0081 to 0.0050. For 17 stories, this improvement rises to 51.41%, with a decrease from 0.0095 to 0.0046. In a 20-story structure, the system remains effective, with a reduction of 47.37%, from 0.0085 to 0.0050. These data indicate that, unlike viscous fluid, viscous walls maintain a more constant control capacity against lateral deformations in tall buildings.

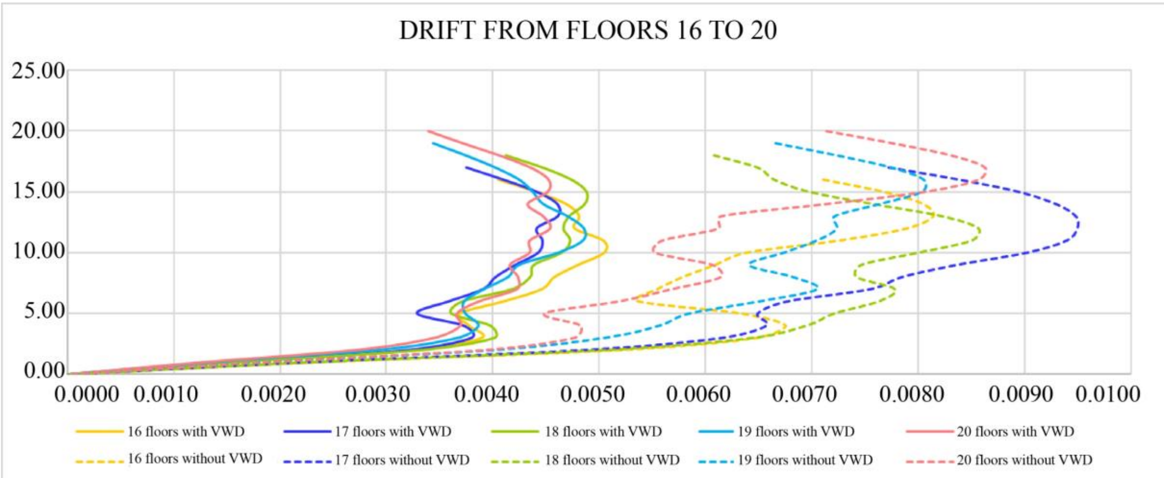

Fig. 24 Viscous wall drift from 16 to 20 stories.

4.3. Acceleration of Viscous Fluid and Viscous Wall

4.3.1. 6 to 10 Stories

Figure 26 shows that viscous fluid dampers achieve significant reductions in the maximum accelerations of buildings, especially on the lower floors. For example, in a 6-story structure, acceleration is reduced from 1.2524 to 0.7709, representing a decrease of 38.45%. This reduction is maintained in intermediate buildings such as the 8-story building, where an improvement of 46.77% is obtained, dropping from 1.7892 to 0.9524. In the case of 10 stories, although the difference is minor, a reduction of 35.35% is still achieved, going from 1.4670 to 0.9484. These results demonstrate the effectiveness of viscous fluid in controlling acceleration, contributing to greater comfort and structural safety in the event of seismic events.

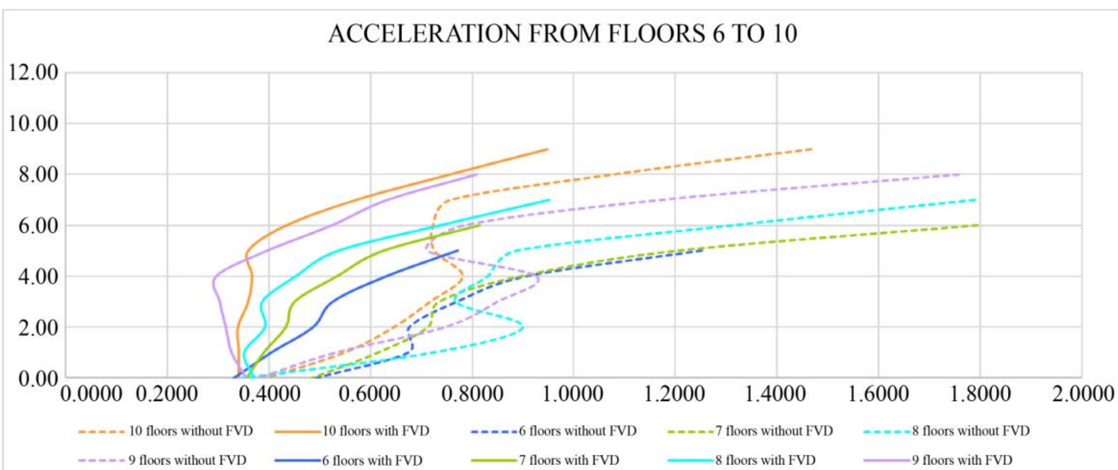

Fig. 25 Acceleration of viscous fluid from 6 to 10 stories

Figure 27 shows that viscous walls also have a favorable influence on reducing maximum accelerations, although to a more moderate extent compared to viscous fluid dampers. In 6-story buildings, the reduction achieved is 13.48%, with a decrease from 1.2587 to 1.0891. For an 8-story structure, the improvement is 18.86%, from 1.7991 to 1.4598. In the case of 10 stories, one of the highest reductions in this category is observed, with 35.76%, dropping from 1.4921 to 0.9585. These data reflect that, although viscous walls are less effective than viscous fluid in terms of acceleration, their performance remains relevant for earthquake-resistant design.

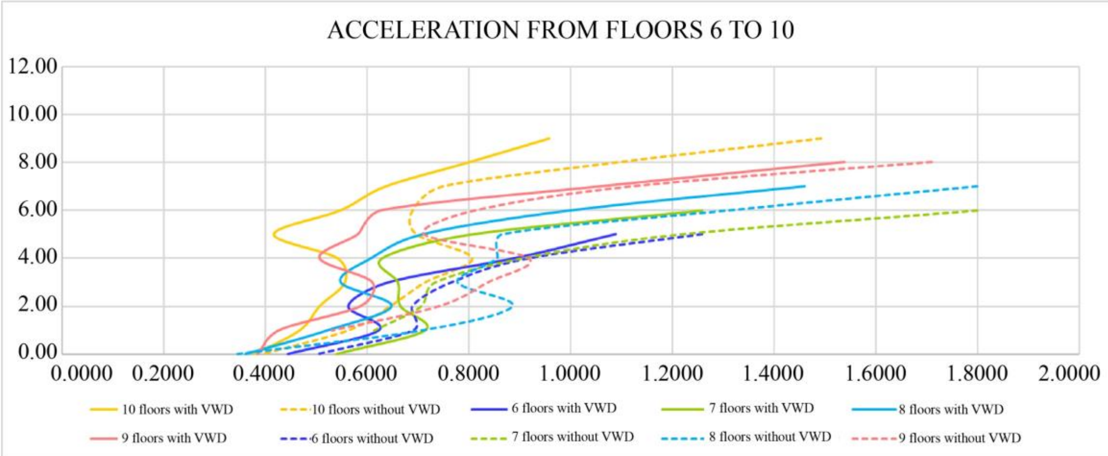

Fig. 26 Acceleration of viscous wall from 6 to 10 stories

4.3.2. 11 to 15 Stories

Figure 28 analyzes the behavior of maximum accelerations in buildings equipped with viscous fluid dampers. The results demonstrate the remarkable effectiveness of these devices in attenuating dynamic responses to seismic loads. In an 11-story structure, the maximum acceleration is reduced considerably from 1.8295 to 0.7091, representing a decrease of 61.60%. This significant reduction indicates a substantial improvement in comfort and structural safety. In intermediate buildings, such as 12-story buildings, the performance remains favorable, achieving a reduction of 65.53%, from 1.7904 to 0.6263. Similarly, in 13-story structures, acceleration decreases from 1.4474 to 0.5471, improving 62.95%. These values show that the implementation of viscous fluid dampers not only improves seismic performance in low- and mid-rise buildings and maintains its effectiveness at higher levels. The attenuation of accelerations minimizes structural and non-structural damage and improves the experience of occupants during a seismic event.

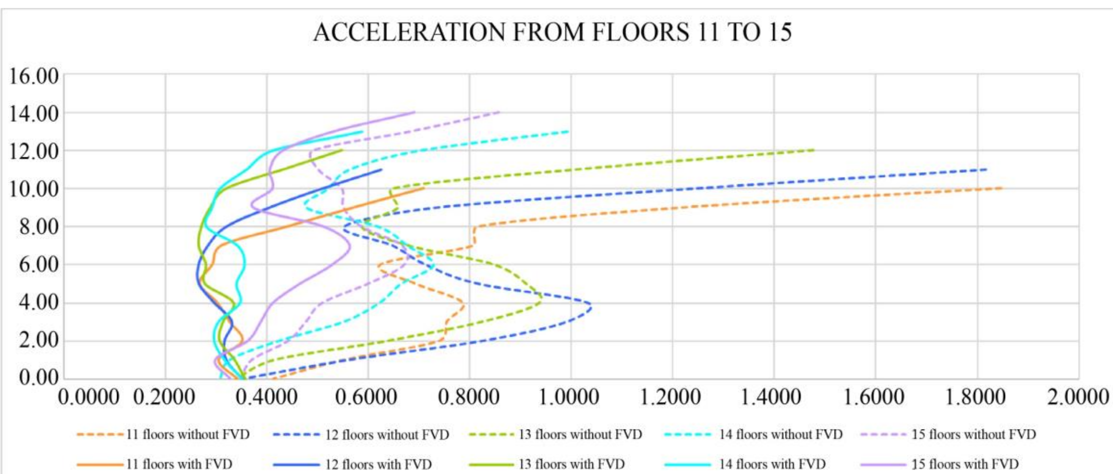

Fig. 27 Acceleration of viscous fluid from 11 to 15 floors

Figure 29 shows the effects of viscous walls on maximum accelerations, demonstrating that they also represent a viable alternative for seismic control, although with relatively lower effectiveness than viscous fluid devices. In an 11-story building, acceleration decreases from 1.1778 to 0.7091, reflecting a reduction of 35.62%. This decrease is significant, as it helps to limit the displacements and stresses induced during an earthquake. For buildings of intermediate height, such as 12-story buildings, a reduction of 32.16% is observed, from 1.2146 to 0.6263. Finally, in taller buildings, such as 13-story buildings, the acceleration is reduced from 1.0022 to 0.5471, achieving an improvement of 30.76%. These results show that viscous walls offer acceptable performance in dissipating seismic energy and reducing accelerations, although their effect decreases as the height of the structure increases. Compared to viscous fluid dampers, viscous walls have a more moderate control capacity, suggesting that their application may be more suitable in projects where a balance between structural efficiency and construction cost is sought.

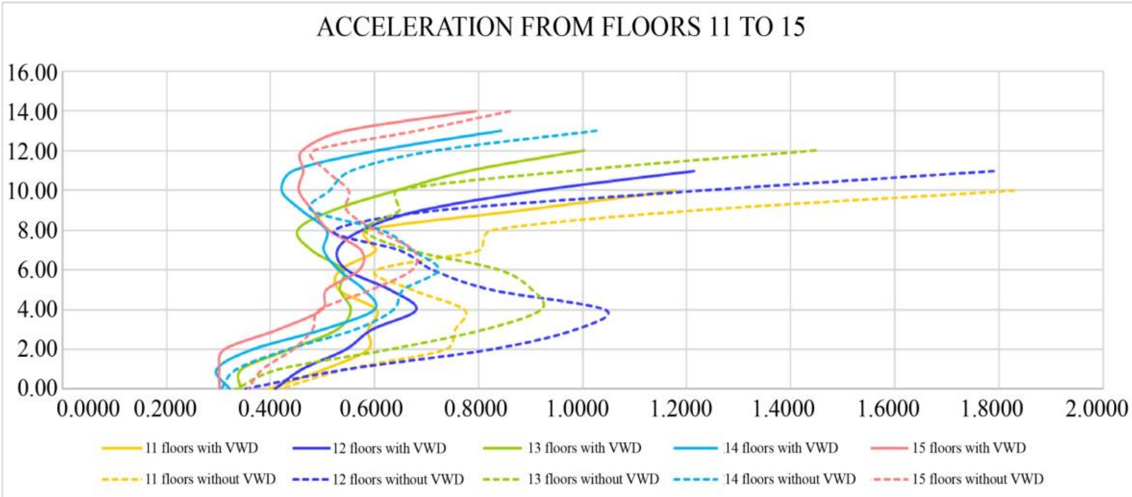

Fig. 28 Acceleration of viscous wall from 11 to 15 stories

4.3.3. 16 to 20 Stories

Figure 30, corresponding to the use of viscous fluid dampers, shows that their effectiveness tends to decrease as the height of buildings increases. For example, in a 16-story structure, there is a reduction in maximum acceleration from 1.0238 to 0.6566, which is equivalent to a decrease of 35.86%, still representing a significant contribution to seismic control. In taller buildings, such as 18-story buildings, the acceleration decreases from 0.9515 to 0.4278, reaching a reduction of 55.04%, which is remarkable considering the dynamic complexity of tall structures. However, in a 20-story building, the effect of viscous fluid becomes marginal: acceleration goes from 1.0534 to 1.0239, representing an improvement of only 2.80%. These results indicate that, although viscous fluid dampers are highly effective in medium-height structures, their efficiency decreases significantly in very tall buildings, possibly due to greater structural flexibility or a change in the dominant vibration mode.

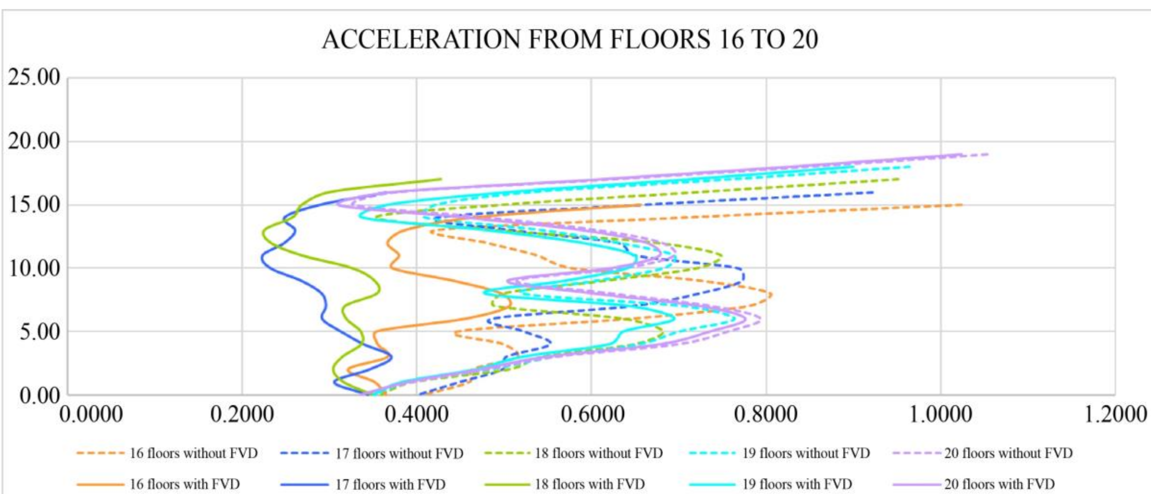

Fig. 29 Acceleration of viscous fluid from 16 to 20 floors

A similar trend is identified regarding the use of viscous walls, shown in Figure 31, although with some particularities. In a 16-story structure, the acceleration is reduced from 1.0030 to 0.6786, achieving a decrease of 32.35%, representing a moderate improvement in dynamic behavior. For 18 stories, the acceleration drops from 0.9245 to 0.7656, achieving a more limited reduction of 17.18%. Finally, in 20-story buildings, a more significant reduction is seen in percentage terms: from 1.0620 to 0.7081, representing an improvement of 33.32%. This behavior suggests that, unlike viscous fluid dampers, viscous walls can maintain more stable effectiveness even at greater heights, possibly due to their rigid integration with the structural system and their ability to contribute to the overall damping of the structure. However, their performance is also affected by the geometry and distribution of the building, so their implementation must be evaluated on a case-by-case basis.

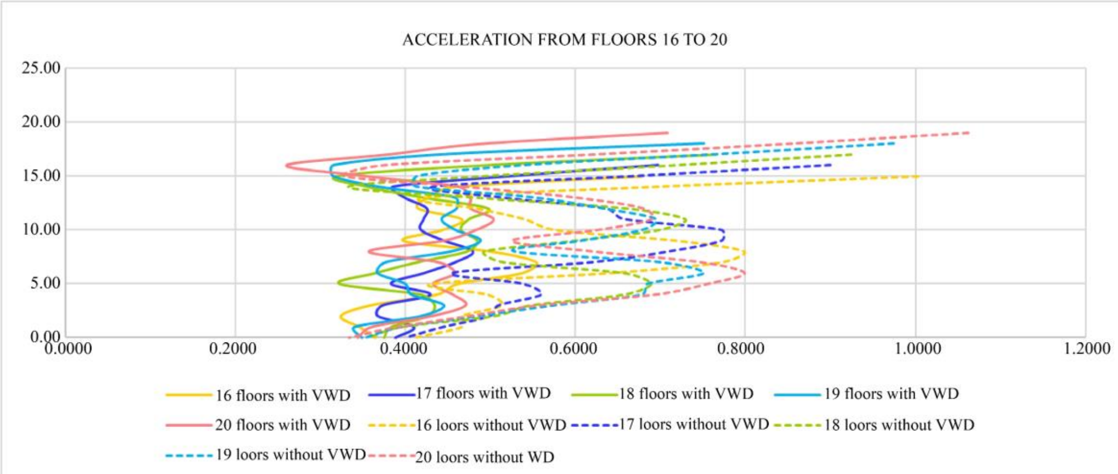

Fig. 30 Acceleration of the viscous wall from 16 to 20 floors

4.4. Shear Force

4.4.1. Viscous Fluid

Figure 32 shows a comparison of the maximum shear force in buildings with and without viscous fluid dampers, from 6 to 20 stories. In general, it can be seen that the use of viscous fluid significantly reduces this force, indicating lower seismic demand on structural elements. In lower buildings, the benefits are notable: in the 6-story building, the shear force is reduced from 2827.77 tons to 2064.22 tons; in the 7-story building, from 2496.98 to 1981.86 tons; in the 8-story building, from 2,864.43 to 1,733.06 tons; and in the 9-story building, from 3,238.45 to 1,437.18 tons. In medium-height buildings, such as those with 10 to 15 floors, there is also a significant decrease: in 10-story buildings, from 2,448.94 to 1,485.36 tons; in 11-story buildings, from 2,519.29 to 1,378.86 tons; in 12-story buildings, from 3,237. 88 to 1387.63 tons; in 13 stories, from 2496.91 to 1415.26 tons; in 14 stories, from 1847.19 to 1380.82 tons; and in 15 stories, from 1554.19 to 1329.89 tons. This trend continues in taller structures such as those with 16 to 18 floors, where considerable reductions are also recorded: in 16-story buildings, from 1,744.77 to 1,081.99 tons; in 17-story buildings, from 2,295.55 to 1,264.99 tons; and in 18-story buildings, from 2,469.07 to 1,370.60 tons. However, in the cases of 19 and 20 stories, the differences are minimal: in 19 stories, it goes from 2029.21 to 1978.82 tons, and in 20 stories, from 2059.71 to 2034.66 tons. This suggests that viscous fluid dampers are highly effective in low- and medium-rise buildings for reducing maximum shear force and improving seismic performance. In contrast, in very tall structures, their effectiveness may be reduced due to the influence of higher vibration modes and the distribution of masses and stiffness.

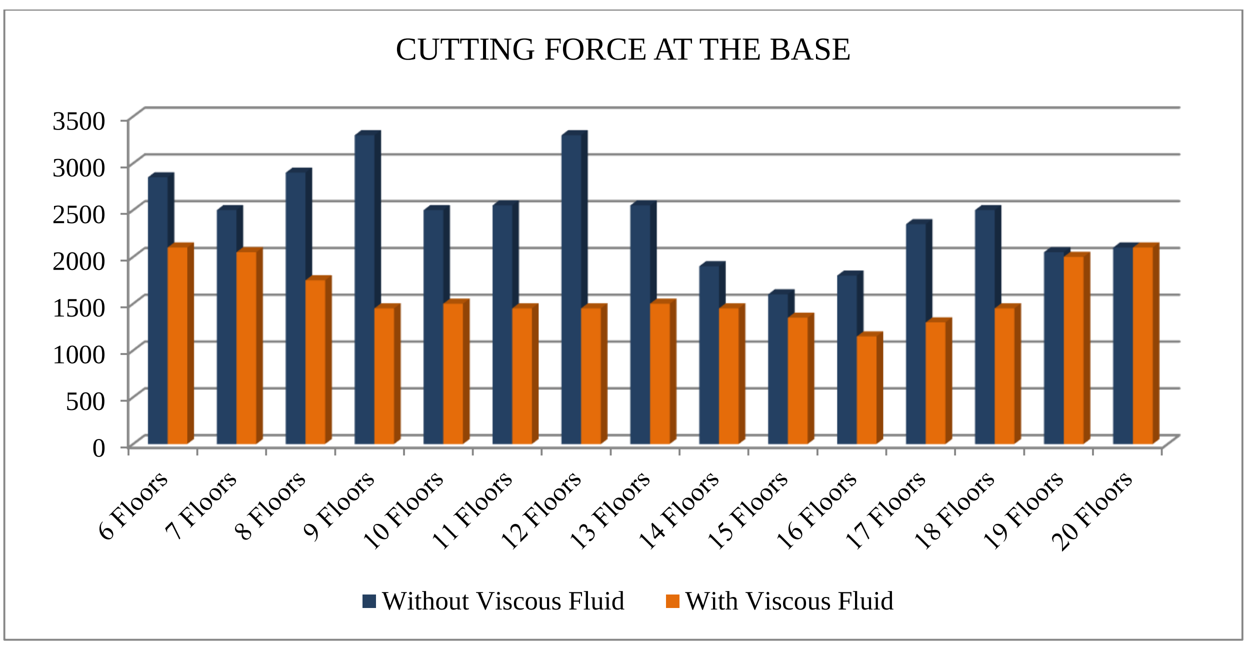

Fig. 31 Viscous fluid acceleration of 16 to 20 floors

4.4.2. Viscous Wall

Figure 33 presents the comparison of the maximum shear force between structures with and without viscous walls in buildings from 6 to 20 stories, showing the positive effect of these elements in the reduction of the seismic demand. In low-rise buildings, an apparent reduction is observed: in 6 stories, the shear force decreases from 2807.59 tons to 2339.41 tons; in 7 stories, it remains almost constant with values of 2470.88 tons without walls and 2479.98 tons with walls; and in 8 stories, it is reduced from 2841.03 to 1962.77 tons. This trend is accentuated in the intermediate floors, such as in 9 stories, where it decreases from 3228.78 to 1955.59 tons; in 10 stories, from 2381.36 to 2033.70 tons; in 11 stories, from 2615.93 to 1674.52 tons; in 12 stories, from 3277.56 to 1658.88 tons; and in 13 stories, from 2428.09 to 1864.50 tons. As the height increases, significant benefits are also observed: at 14 stories, from 1867.37 to 1817.61 ton; at 15 stories, from 1545.62 to 1464.13 ton; at 16 stories, from 1775.39 to 1099.27 ton; at 17 stories, from 2327.86 to 1051.17 ton; at 18 stories, from 2471.15 to 1414.78 ton; at 19 stories, from 2031.00 to 1333.55 ton; and finally at 20 stories, from 2080.65 to 1512.40 ton. These results confirm that viscous walls are effective at all heights analysed, achieving significant reductions in the maximum shear force and, therefore, improving the structural capacity against seismic loads.

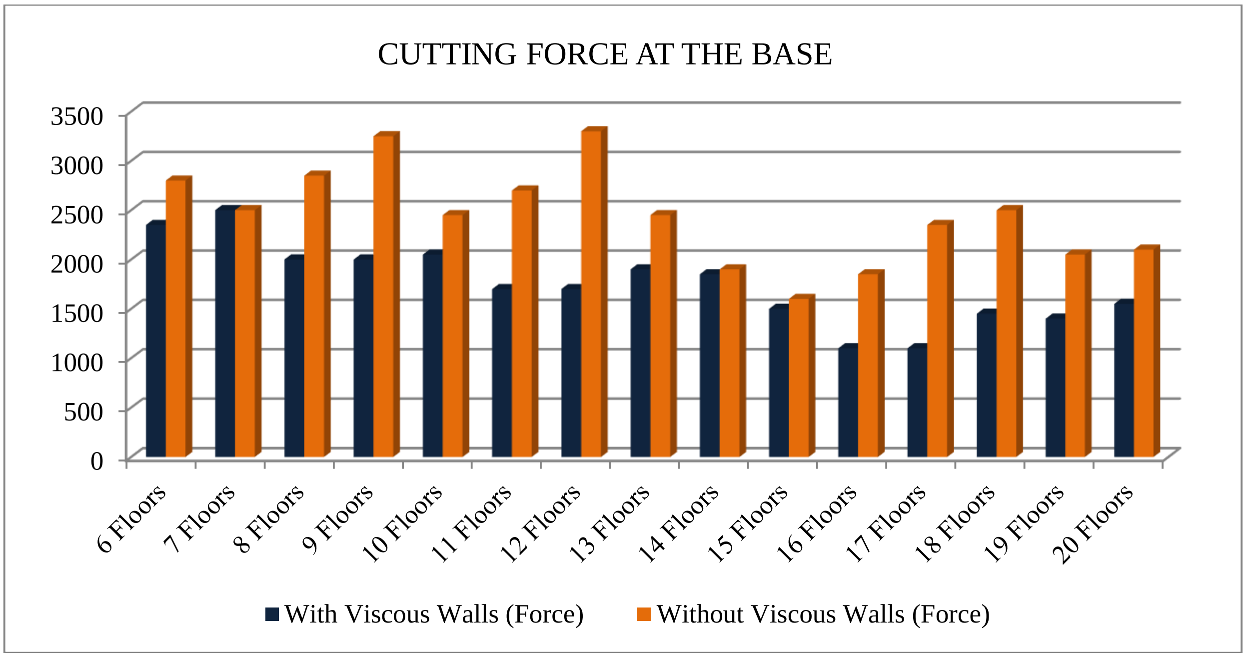

Fig. 32 Viscous wall acceleration of 16 to 20 floors

4.5. Stresses in the Intervened Axis

4.5.1. Framework Analysed

Figure 34 shows the sketch corresponding to axis 2 of the 20-storey building, which was evaluated under three structural configurations: without a wall and viscous fluid, with viscous fluid, and with a viscous wall.

In this sketch, the main elements of the structural frame were clearly identified, such as the left column (C52), the beam (B134), and the right column (C59), as well as the viscous wall W6, located on the right side of the frame in the models where this element was included.

These numberings allowed the systematic extraction of the stress information for each element, which facilitated the comparative analysis of the structural behaviour of the building.

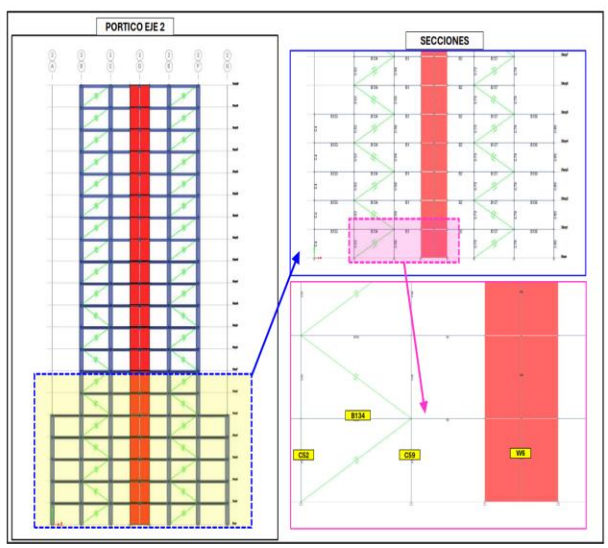

Fig. 33 Sketch of axis 2 analysed

4.5.2. Axial Force on the Frame

Table 5 presents the axial force values extracted from the structural elements detailed in the sketch, specifically the columns C52 and C59 of the frame, the beam B134, and the slurry wall W6. The evaluation was carried out for the three configurations: without devices, with viscous fluid, and with viscous wall.

Figure 35 showed that the axial force increased significantly for columns C52 and C59 as the number of storeys increased. This increase was attributed to the progressive accumulation of gravity loads together with the amplified seismic response in taller buildings. This phenomenon was especially critical in the configuration without dissipation devices: for a 20-storey building, the C59 column reached up to 329.72 tonnes in compression. Such a demand represents a considerable challenge for stability since under cyclic loading conditions, buckling or loss of resistance capacity could be favoured if the design does not ensure adequate ductility and confinement.

With the incorporation of viscous fluid devices, a significant reduction in the axial forces of the columns was observed. For example, in the case of 20 storeys, the axial load in C59 was reduced to approximately 114.28 tonnes, and in C52 it dropped to 81.95 tonnes. This decrease was explained by the dissipative action of the viscous fluid, which attenuated the inter-storey displacements and, consequently, limited the transfer of forces to the structural frame. This effect not only increased the overall safety of the system but also facilitated a more efficient design of the vertical elements.

In the viscous wall system, the structural behaviour changed significantly. The W6 wall began to assume a significant proportion of the axial load, exceeding 119.29 tonnes in the 20-storey building. In parallel, columns C52 and C59 kept their axial forces under control in ranges between 132 and 166 tonnes, depending on the height. This result evidenced an efficient transfer of the seismic load to the viscous wall, which functioned as the main resisting element of the system against axial forces, thus relieving the frame from excessive demands and potential compressive failure mechanisms.

In summary, the results obtained showed that the introduction of dissipation devices, and especially the viscous wall, promoted a more favourable distribution of axial forces, improving the safety and structural performance of the building under gravity and seismic loads.

Table 5. Axial force in the models analysed

Floors	Axial without devices (ton)				Axial with Viscous Fluid (ton)				Axial with Viscous wall (ton)			
20	155.7860	0	184.5959	187.9770	153.2763	0	182.4669	186.4057	171.4548	0	187.6348	145.8931
19	195.6345	0	231.1376	197.9999	193.3573	0	224.4372	195.5559	189.6242	0	223.7878	155.8070
18	268.4841	0	328.9215	221.9044	162.9952	0	216.0345	165.7578	193.0140	0	237.2352	157.2858
17	266.4629	0	351.0760	211.5957	82.2314	0	112.5013	74.1343	182.1509	0	210.2662	124.9486
16	218.6082	0	276.8620	196.4083	191.1671	0	253.4552	174.6318	172.1039	0	211.0419	118.7195
15	220.3821	0	278.2132	191.2574	185.3742	0	237.4300	154.2341	145.1473	0	169.8710	108.1960
14	181.2138	0	253.7591	139.0564	115.4349	0	143.8328	90.6564	160.4412	0	199.0000	109.9369
13	229.1082	0	329.7150	145.6575	81.9545	0	114.2833	65.2942	132.5706	0	166.7615	119.2942
12	193.0322	0	298.4796	115.9927	64.0694	0	98.6328	53.3959	88.5914	0	120.2548	57.9288
11	126.1901	0	229.7374	76.8257	53.2698	0	98.8149	46.6460	59.5886	0	107.2386	51.9113
10	65.9397	0	137.7624	54.4932	44.3451	0	95.6915	40.6591	48.5745	0	112.5724	44.9027
9	58.8508	0	164.0549	61.4635	36.2607	0	108.9132	30.8074	44.3327	0	93.2045	48.7433
8	41.3541	0	153.4636	36.2757	29.1482	0	113.9698	22.6641	33.1689	0	127.3875	29.0540
7	23.3998	0	127.7123	20.1990	19.4354	0	104.3738	12.5647	25.9653	0	121.9747	16.2099
6	13.1805	0	126.0931	10.0164	9.7561	0	98.5725	6.8568	15.8636	0	109.4359	8.9482
	C52	B134	C59	W6	C52	B134	C59	W6	C52	B134	C59	W6

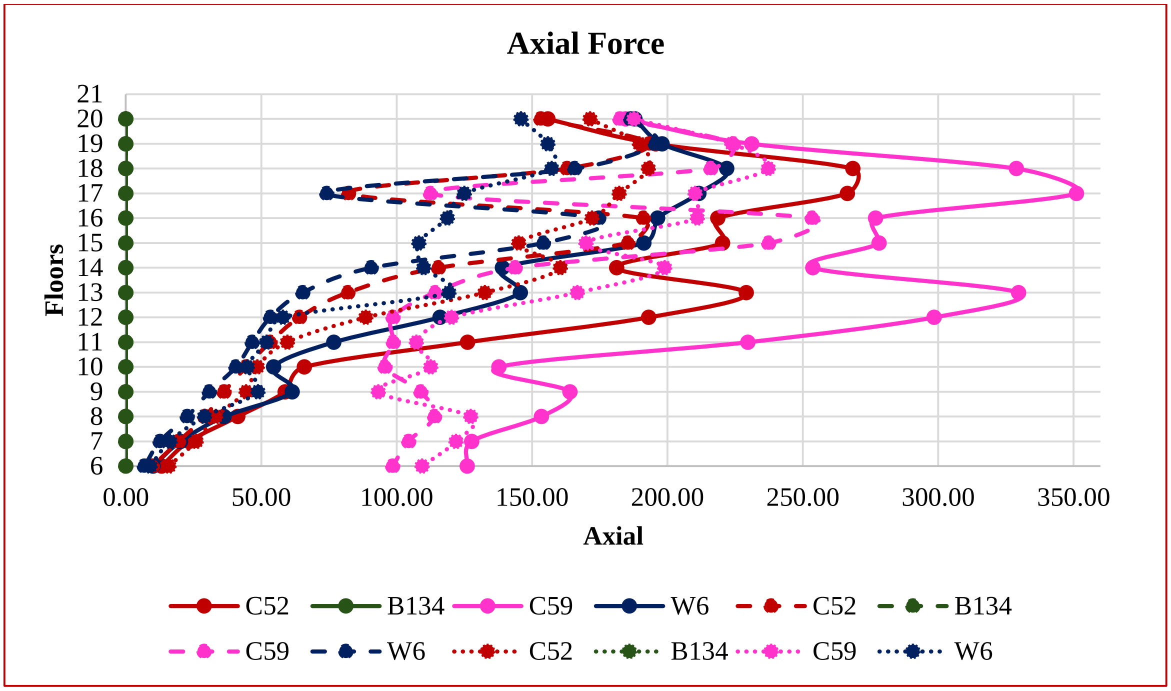

Fig. 34 Axial force on frame members

4.5.3. Moment 3-3

Table 6 compiled the 3-3 bending moment values extracted from the structural elements shown in the sketch, focusing on columns C52 and C59, beam B134, and slurry wall W6. The analysis covered the three structural configurations: without control devices, with viscous fluid, and with viscous wall.

Figures 36 and 37 illustrate the bending distribution in the plane of the portal frame under lateral loads. In the model without dissipation systems, it was evident that the moments 3-3 increased dramatically with the height of the building. For the 20-storey structure, column C59 developed maximum moments up to 177.38 ton-m, while 172.97 ton-m were recorded in C52. These high values are representative of high rotation at the column bases, which increases the risk of unwanted plastic hinge formation and thus structural failure under severe seismic events.

The introduction of viscous fluid devices resulted in a significant reduction of the 3-3 moments in the frame elements. For example, at storey 20, the 3-3 moment at C59 decreased to 82.03 ton-m and at C52 to 79.20 ton-m. This reduction allowed the deflections to remain within the elastic or ductile range of the material, increasing the structural safety and energy dissipation capacity under seismic loads.

On the other hand, in the viscous wall model, a different behaviour was observed in the moment distribution. While column C59 maintained a considerable 3-3 moment of approximately 124.47 ton-m, the viscous wall W6 assumed most of the flexural demand, reaching values of more than 4277.38 ton-m. This showed that the wall not only provides stiffness to the system, but also behaves as the main energy dissipator, absorbing most of the moment induced by the seismic forces and relieving the frame from extreme bending stresses.

In conclusion, the results showed that both the use of viscous fluid and the implementation of viscous walls proved to be highly effective strategies to limit the magnitude of bending moments in the frame elements. The viscous wall, especially, concentrated most of the energy, preventing the formation of unwanted plastic mechanisms in the columns, thus optimising the safety and seismic performance of the structure.

Table 6. Bending moment in the models analysed

Floors	Axial without devices (ton)				Axial with Viscous Fluid (ton)				Axial with Viscous wall (ton)			
20	91.4502	-10.0242	93.7266	3233.2889	89.1153	-9.7874	91.3358	3155.1793	76.0411	-8.6605	77.9333	2729.5144
19	105.0676	-11.7965	107.7423	3779.7638	101.5421	-11.4153	104.1298	3656.4451	83.6536	-9.4573	85.7431	2988.1592
18	131.9838	-14.8702	135.3576	4760.1253	69.0331	-7.5562	70.8209	2438.2623	96.1814	-10.5561	98.5742	3379.2010
17	128.4201	-14.2523	131.7313	4582.8313	51.6174	-5.4994	52.9287	1779.2520	95.3033	-10.6718	97.6098	3305.6605
16	131.0492	-14.4661	134.4487	4660.4162	112.7351	-12.3708	115.6257	3988.5087	95.7187	-10.4623	98.0763	3357.6509

15	127.1090	-13.7224	130.3206	4440.9809	116.6053	-12.6113	119.5506	4079.1208	94.7070	-10.0843	96.9673	3255.1051
14	122.4747	-13.1530	125.5298	4257.2208	67.1371	-7.3193	68.8627	2366.6301	89.3278	-10.0989	91.5948	3195.1542
13	111.2688	-12.6247	114.1877	4034.9271	80.0319	-8.5845	82.0259	2785.3926	121.4953	-13.9920	124.4689	4277.3816
12	172.9771	-19.2274	177.3822	6173.1710	79.2077	-8.5196	81.1484	2751.2789	119.2733	-13.3533	122.1266	4107.7411
11	171.1241	-14.2420	174.5671	6077.9093	82.5322	-6.9874	84.1965	2971.8659	114.9053	-9.4698	117.0891	3994.5744
10	136.5421	-10.8992	139.1797	4719.0560	90.8694	-7.5483	92.6722	3212.7272	100.3591	-8.6908	102.4257	3647.8794
9	149.8272	-12.5902	152.9105	5373.7592	89.1255	-7.4578	90.9391	3186.4072	112.0082	-6.9513	121.4967	2914.9247
8	139.9797	-11.2528	142.7286	4864.5873	79.4292	-6.7873	81.0357	2830.2804	97.4379	-8.3763	99.3338	3494.0437
7	113.1333	-10.1139	115.6107	4239.1717	96.0770	-8.4286	98.1388	3545.3819	119.6366	-10.2797	122.0290	4263.8522
6	152.3486	-13.1450	155.5690	5557.4744	119.9979	-10.2195	122.5012	4339.9789	149.3644	-12.9671	152.3469	5340.8236
	C52	B134	C59	W6	C52	B134	C59	W6	C52	B134	C59	W6

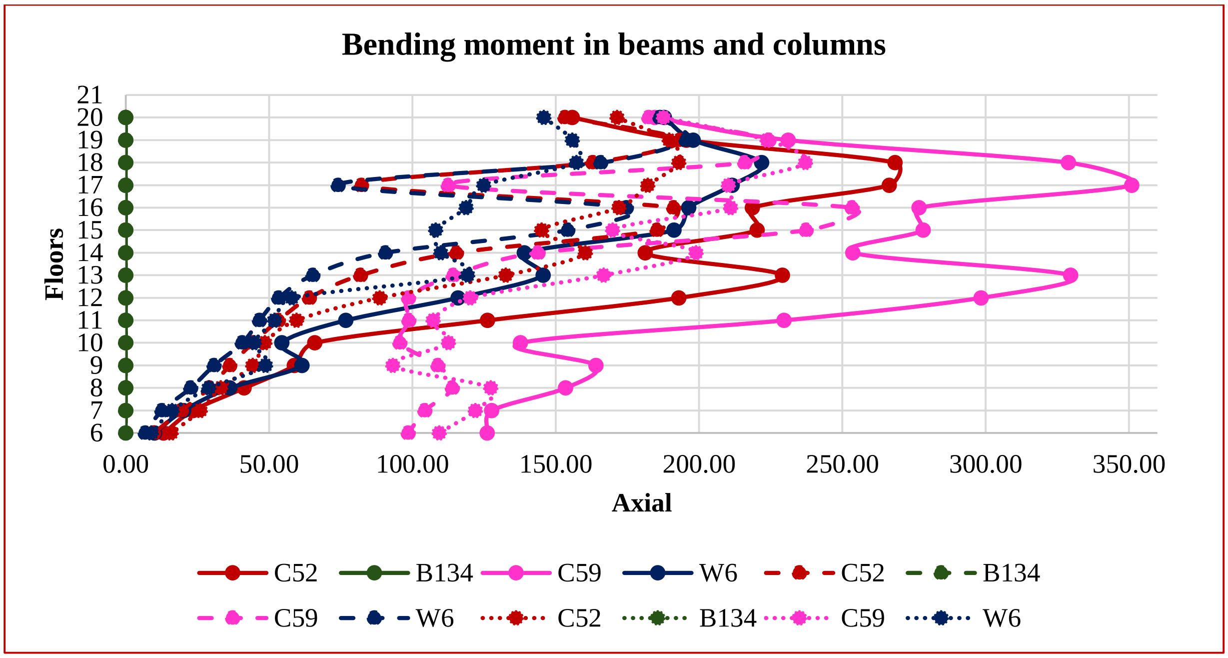

Fig. 35 Bending moment on frame members

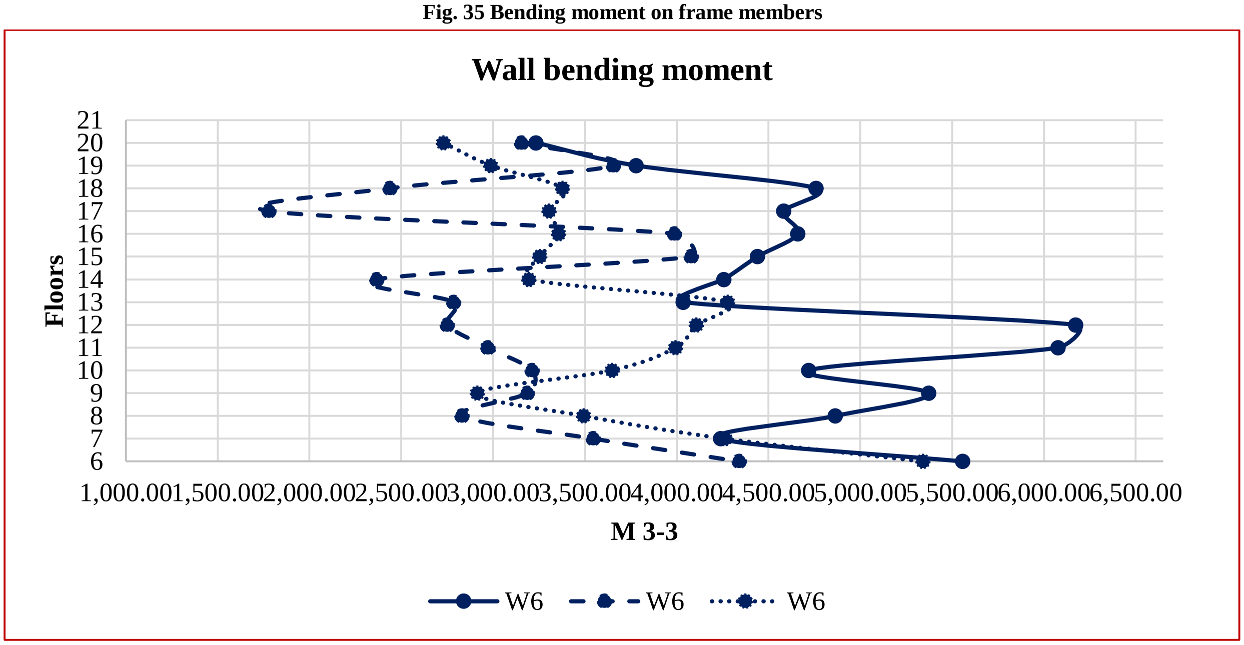

Fig. 36 Bending moment in the frame resisting elements

4.5.4. Shear

Table 7 presents the shear values extracted from the structural elements detailed in the sketch, specifically columns C52 and C59, beam B134, and slurry wall W6. The analysis considered three structural configurations: without control devices, with viscous fluid, and with viscous wall.

In Figures 38 and 39, corresponding to the system without control devices, it was observed that the shear values increased considerably with the height of the building, reaching maximum values of 43.14 tonnes at column C59 and 38.27 tonnes at column C52 for 20-storey buildings. This behaviour indicates a significant risk of brittle shear failure in the columns, especially if an adequate amount of transverse reinforcement is not designed to resist such stresses.

The incorporation of viscous fluid devices resulted in a noticeable reduction of the V2-2 shear stress in the frame elements. For example, for column C59, the shear decreased to 21.35 tonnes, while in C52 it decreased to 19.31 tonnes. This decrease significantly improves the seismic performance of the columns, as it reduces the demand for transverse reinforcement and decreases the probability of shear failure.

On the other hand, the inclusion of a viscous wall significantly modified the shear distribution within the structural system. In this case, the W6 wall absorbed most of the V2-2 shear force, concentrating up to 592.77 tonnes in 20-storey buildings, while the shear in the frame columns was reduced to values below 28 tonnes. This behaviour is evidence of an efficient transfer of lateral forces to the wall, which is the element specifically designed to absorb these forces, thus avoiding overloading of vertical elements not designed for shear.

In summary, the results show that the implementation of control devices, especially the viscous wall, is highly effective in redistributing and reducing the shear forces in the critical elements of the structural frame, significantly improving the safety and seismic performance of the building.

Table 7. Shear in the models analysed

Floors	Axial without devices (ton)				Axial with Viscous Fluid (ton)				Axial with viscous wall (ton)			
20	20.5868	7.4396	23.1482	436.4341	19.9801	7.2638	22.4787	423.2837	16.3878	6.8767	18.5169	342.9283
19	22.4639	8.7569	25.4735	472.3026	21.6457	8.4738	24.5574	454.9041	18.2924	7.5075	20.6436	384.0463
18	28.1045	11.0409	31.9008	590.6405	16.0978	5.6197	18.0590	344.4215	22.1114	8.3401	24.7501	469.6670
17	28.1180	10.5921	31.8438	595.0592	12.4465	4.0484	13.9219	267.5560	22.6727	9.1729	25.2680	479.2888
16	28.9757	10.7534	32.8009	615.5661	25.3125	9.1958	28.5650	538.1094	22.0643	8.2463	24.7023	468.4985
15	29.5738	10.2010	33.1875	631.2262	27.0347	9.3750	30.3487	576.8652	23.0538	9.9398	25.5971	491.6100
14	29.3117	9.7794	32.6928	627.0169	16.4760	5.4365	18.2632	354.8629	19.6902	8.0111	22.1855	416.0035
13	25.7226	9.3768	28.5012	553.1682	19.0046	6.3728	21.1210	406.0728	28.1901	12.1052	31.5361	592.7702
12	38.2733	14.2770	43.1462	810.7380	19.3149	6.3255	21.3561	412.2484	28.9422	11.5693	32.1527	610.9153
11	38.5257	9.9106	42.3610	823.2933	19.3832	4.8612	21.1350	416.7890	27.9392	7.3115	30.3718	599.9984
10	33.1436	7.5728	36.0817	711.8054	21.1593	5.2485	23.1108	453.4236	24.2228	6.4404	26.1467	521.8641
9	32.8770	8.7557	36.2083	708.9377	19.6952	5.1827	21.7154	419.0201	25.2747	5.1897	26.8712	361.0797
8	33.4585	7.8230	36.5205	720.4243	17.7509	4.6300	19.5404	375.7351	22.7612	6.2079	24.8731	483.9439
7	23.5578	7.0401	25.7564	503.5245	20.5221	5.8701	22.7322	434.0578	27.2307	7.9500	29.6765	579.6140
6	31.6143	9.1595	35.2017	672.5884	26.2527	7.1166	28.8946	557.3536	34.4180	10.4862	37.6668	726.1812
	C52	B134	C59	W6	C52	B134	C59	W6	C52	B134	C59	W6

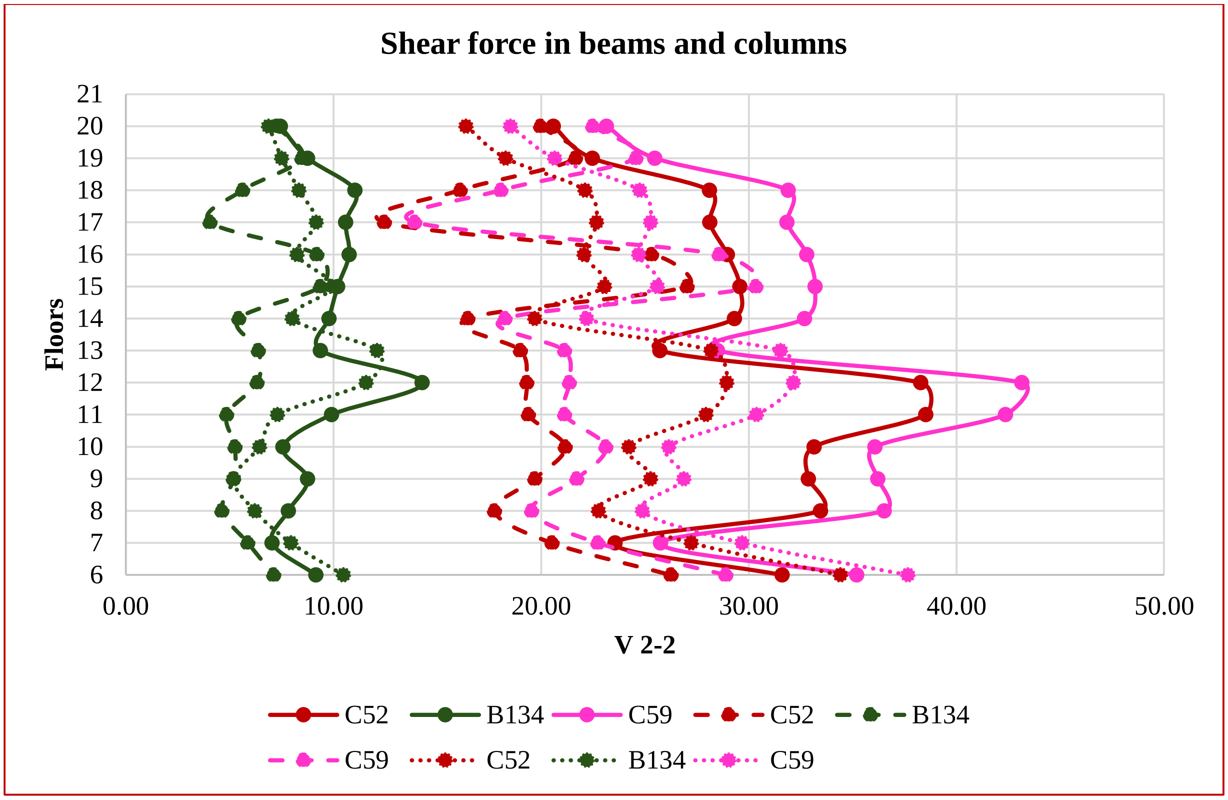

Fig. 378 Shear force on frame members

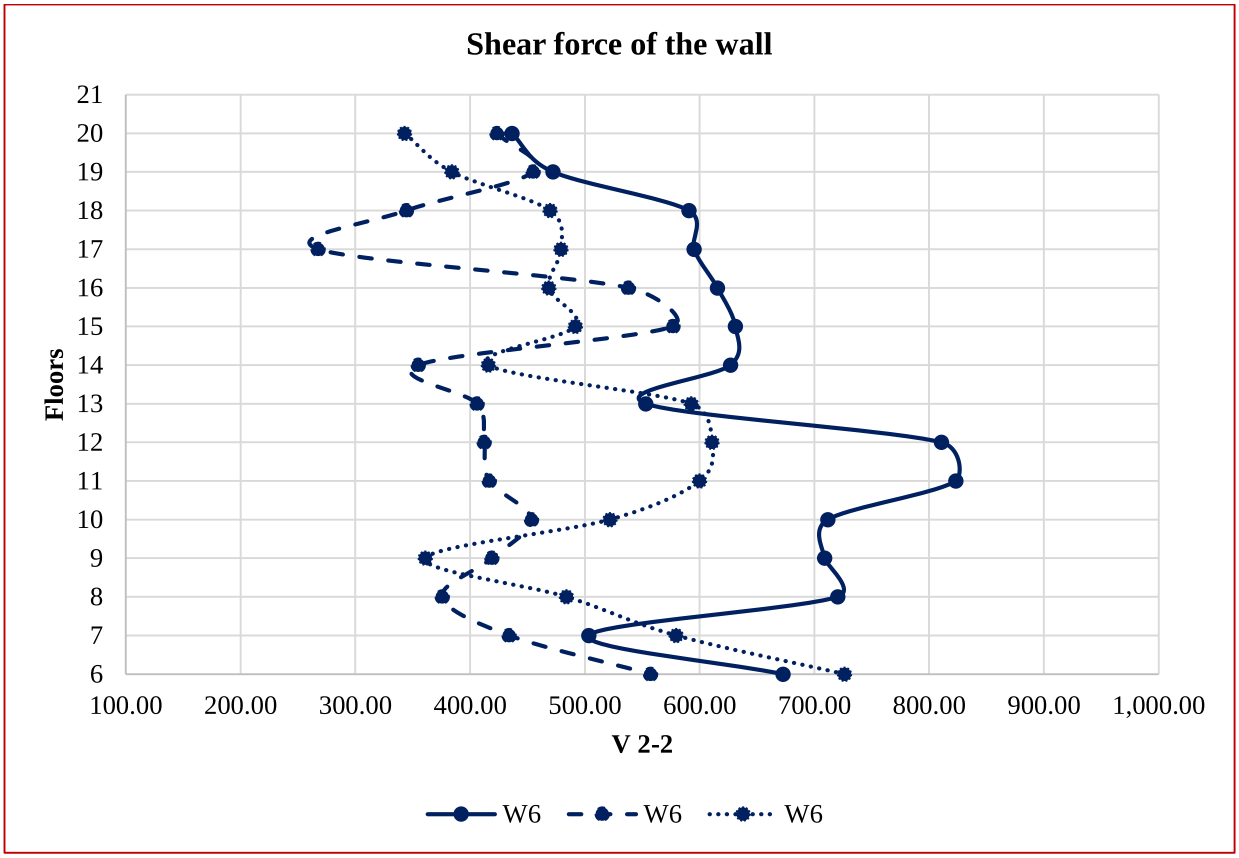

Fig. 38 Shear force on frame members

5. Discussions

According to Hidayaty et al. [37], in their research, they evaluated the performance of viscous wall dampers in a steel structure subjected to three types of earthquakes. The results showed a significant reduction in displacement in the structure. In the X and Y directions, displacement was reduced by 50.78%, while in the Y direction alone, it was reduced by 23.96%. In addition, a decrease in the periods of the structure was observed, as well as an improvement in the dynamic response, reducing displacements, velocity, and acceleration. These findings suggest that the implementation of viscous wall dampers can be effective in significantly mitigating structural damage caused by seismic loads, improving the overall performance of the structure during a seismic event. Furthermore, according to author P. Katsimpini [35], in his study, they analyzed the performance of viscous wall dampers in a four-story structure subjected to both individual and consecutive seismic events. The results showed that implementing these dampers significantly reduced inter-story drifts (IDR). On the first floor, the maximum IDR was reduced to 0.62% for sequential movements and 0.6% for individual movements. On the second floor, the reductions were 0.59% and 0.57%, respectively. The third floor showed a decrease to 0.4% and 0.39%, and the fourth floor achieved the lowest drifts, with values of 0.33% for sequential movements and 0.31% for individual movements. This analysis highlights the ability of viscous wall dampers to improve structural stability in the face of seismic movements. Based on these results, this study supports the idea that the incorporation of viscous walls in buildings contributes significantly to the reduction of drifts, achieving a maximum decrease of 51.41% on the 17th floor, which reinforces the effectiveness of this technology in structures subjected to seismic loads.

According to the authors, Fk. Lawmzela and Gagandeep Singh [39], in their study they analyzed the seismic performance of 15-story buildings with square, L-shaped, and O-shaped layouts equipped with viscous fluid dampers (FVD) and Lead Rubber Bearings (LRB). The FVDs reduced the fundamental period of the structure by 52.7% for the square shape and 57.7% for the L- and O-shaped buildings. In addition, the FVDs reduced the maximum floor displacement by up to 57.12%, the inter-story drift by up to 61.8%, and the base shear by between 93.3% and 96.6%. In contrast, LRBs increased the maximum floor displacement, inter-story drift, and fundamental period, but reduced the base shear stress between 27.4% and 34.7%. The combined system showed moderate effectiveness, reducing the period time compared to the non-damped cases but increasing it compared to the FVDs separately. Consistent with this research, the results of the present study confirmed significant improvements. Similar trends were identified, although different geometric conditions were analyzed, specifically vertical geometric irregularities instead of square, O-shaped, or L-shaped configurations. The models exhibited up to 74.42% reduction in maximum displacements on floor 17, a 70.02% reduction in drift at the same level, and a 57% decrease in shear stress on floor 12. These results confirm the coherence of the methodology with previous studies and highlight the critical role of control devices in vertically irregular buildings.

6. Conclusion

In conclusion, with regard to maximum displacement, viscous fluid dampers demonstrated exceptional performance in reducing lateral displacement, with outstanding efficiency in 12-, 13-, and 14-story buildings, achieving reductions of 57.99%, 57.89%, and 57.30%, respectively. The largest reduction recorded, 74.42%, was obtained in a 17-story structure, highlighting its effectiveness in tall buildings. On the other hand, viscous walls also showed significant performance, especially in 12- and 17-story structures, with reductions of 47.79% and 55.75%, respectively. These results demonstrate that both technologies offer efficient control of structural displacement, with viscous fluid dampers being the most effective in most cases analyzed, especially in medium and tall buildings, improving structural stability and functionality in the face of seismic movements.

In terms of maximum drifts, viscous fluid dampers were highly effective in controlling angular displacement between floors, with reductions of over 50% at several levels. The 11-, 12-, 13-, and 17-story structures showed efficiencies of 50.37%, 58.68%, 57.43%, and 70.02%, respectively, with the latter being the most notable. Viscous walls also had a considerable impact, especially in 17- and 20-story buildings, with reductions of 51.41% and 47.37%, respectively. These results confirm the effectiveness of both systems in mitigating drifts, with viscous fluid dampers being the most efficient in most cases, especially in medium and tall structures, strengthening the structural response to seismic actions.

In terms of maximum accelerations, it was observed that viscous fluid dampers have a significant impact on reducing the dynamic response of buildings to seismic movements, with reductions of more than 60% in 11-, 12-, and 13-story buildings, achieving efficiencies of 61.60%, 65.53%, and 62.95%, respectively. These results reflect a remarkable capacity for energy dissipation, especially in mid-rise structures. Viscous walls also performed well, particularly in 10-, 11-, and 16-story structures, with reductions of 35.76%, 35.62%, and 32.35%, respectively. This confirms the effectiveness of both systems in mitigating structural accelerations, with viscous fluid devices being the most efficient, especially in mid-rise buildings.

Finally, in the analysis of shear forces, viscous fluid dampers showed notable reductions, especially in buildings with 8 to 18 floors, where the shear force decreased from 2,864. 43 tons to 1,733.06 tons in 8 stories and from 2,469.07 tons to 1,370.60 tons in 18 stories, representing significant improvements in structural response to earthquakes. Viscous walls also showed considerable improvement, with significant reductions in 12-story structures (from 3277.56 to 1658.88 tons) and 17-story structures (from 2327.86 to 1051.17 tons). Together, both passive technologies provide significant benefits in mitigating seismic forces, making them highly recommended tools for earthquake-resistant design, particularly in medium- to high-rise structures, where their effects are more pronounced and consistent.

Based on a detailed analysis of the internal forces within the structural frame of the 20-story building, it was found that the incorporation of control devices, especially viscous walls, generates a notable redistribution of forces within the structure. The results showed that, when a viscous wall was implemented, both the axial and shear forces and the bending moments in the frame columns decreased considerably. Wall W6 became the central receiver of lateral and axial loads, absorbing most of the seismic energy and relieving the columns and beams of excessive demands. This behavior demonstrates the potential of viscous walls not only as elements of rigidity but also as primary energy dissipators, which directly contribute to the protection of vertical elements against failure due to shear, compression, or bending. On the other hand, the results also revealed that viscous fluid dampers, although highly effective in reducing overall displacements, drifts, and accelerations, did not redistribute internal stresses in the same way as viscous walls. However, the significant reduction in maximum stresses in columns achieved with both systems significantly reduces the risk of plastic hinge formation and buckling under cyclic loads, thereby improving ductility and structural resilience in the event of severe seismic events.

This study provided quantitative evidence on the importance of analyzing not only global displacements but also the internal response of key structural elements. The approach of systematically extracting and comparing axial, shear, and bending forces in the main components of the frame allowed for the objective identification of the benefits of each control system, providing a solid basis for the selection of earthquake-resistant design strategies. Thus, it highlights the need to choose or combine control technologies according to the specific demands of the project, prioritizing both global stability and local protection of the most stressed elements.

Finally, these findings broaden the scope for structural design in high-rise buildings, demonstrating that the integration of control devices, particularly viscous walls, can be decisive in achieving safe and efficient structural performance. Furthermore, this type of analysis opens the door to innovative proposals for hybrid solutions, in which optimal synergy is achieved between displacement reduction and favorable redistribution of internal forces, thus maximizing the safety and seismic performance of the building. Future research could focus on several key aspects to improve the analysis and implementation of structural control devices. Studies involving nonlinear dynamic analysis and time-history simulations with multiple seismic records are recommended to evaluate structural behavior under more realistic and extreme conditions. In addition, the interaction between shear forces, displacements, and drifts should be further investigated to understand better how control devices affect the distribution of forces throughout the structure. The optimization of control devices should also be an area of interest, extending the analysis to other passive and active systems, including hybrid systems, to compare their effectiveness in reducing accelerations, shear forces, and displacements. It is also recommended that parametric studies be conducted on different wall and damper configurations to explore how their location and quantity affect structural behavior. Research could include full-scale or reduced-scale experimental tests to validate the results obtained numerically and compare the performance of theoretical models with actual models. In addition, it would be important to evaluate the impact of control devices on comfort and non-structural safety, considering elements such as internal partitions, glass, and equipment sensitive to movement. Finally, an analysis of the long-term behavior of dissipators is suggested, evaluating their durability, effectiveness, and possible failures due to material fatigue and repeated seismic cycles.

6.1. Practical Implications and Professional Recommendations

This research demonstrates that the incorporation of viscous dampers should not only be seen as a theoretical improvement but as a practical tool for earthquake-resistant design in regions of high seismic hazard. From a professional perspective, the results provide actionable insights: viscous fluid dampers are most efficient for reducing global response parameters such as displacements, drifts, and accelerations, while viscous wall dampers are particularly effective in redistributing internal forces and protecting critical load-bearing elements. For design engineers, this implies that the choice between FVDs and VWDs must consider the building height, irregularity, and structural priorities. FVDs offer greater global control in medium-rise buildings, whereas in tall buildings with vertical irregularities, VWDs provide a crucial safeguard against overstressing of columns and walls. Practitioners are therefore advised to adopt a combined strategy, integrating both systems to maximize overall resilience.

It must also be emphasized that the ethical dimension of structural safety is fundamental: the integration of reliable energy dissipation systems directly translates into the protection of human lives, the reduction of economic losses, and the preservation of essential infrastructure functionality after major earthquakes. Consequently, seismic design should not be limited to code compliance but should adopt advanced damping technologies as a professional responsibility toward public safety.

6.2. Practical Implications and Professional Recommendations

In structural engineering, the ethical dimension is inseparable from the design and implementation of seismic control devices. The foremost responsibility is public safety: every structural decision must prioritize protecting human life. Using viscous fluid dampers and viscous wall dampers is not only a technological choice but an ethical obligation in highly seismic regions. From a professional standpoint, engineers must ensure the rigorous selection of seismic records, accurate modeling, and transparent communication of assumptions and limitations. Any omission or manipulation of data can compromise safety and undermine public trust. Furthermore, ethical practice requires consideration of long-term performance, including the durability and maintenance needs of damping devices, to avoid premature failures that could place occupants at risk. Ultimately, ethical responsibility in earthquake engineering lies in guaranteeing that solutions comply with standards, are based on verified scientific evidence, and never prioritize cost savings over safety. In seismic-prone contexts such as Lima and the central coast of Peru, engineers must deliver structural solutions that reduce vulnerability, protect lives, and reinforce confidence in the profession.

Acknowledgments

The authors wish to express their sincere thanks to Marko Antonio Lengua Fernández for his valuable advice, guidance, and comments for improvement during the research process.

References

[1] Number of Earthquake Fatalities Recorded Worldwide from 2000 to 2021. [Online]. Available: https://es.statista.com/estadisticas/635156/numero-de-muertes-provocadas-por-terremotos-a-nivel-mundial/

[2] Number of earthquakes of magnitude 5 or greater on the Richter scale recorded worldwide from 2000 to 2023. [Online]. Available: https://es.statista.com/estadisticas/635155/numero-de-terremotos-registrados-a-nivel-mundial/

[3] The Reason Why Peru, Chile and Mexico, Among other Latin American Countries, Suffer Tremors and Earthquakes, La República, 2024. [Online]. Available: https://larepublica.pe/mundo/2024/11/07/la-razon-por-la-que-peru-chile-y-mexico-entre-otros-paises-de-america-latina-sufren-temblores-y-terremotos-548988

[4] The Geophysical Institute of Peru reported more than 500 earthquakes in 2019, Geophysical Institute of Peru. [Online]. Available: https://www.gob.pe/institucion/igp/noticias/71381-mas-de-500-sismos-reporto-el-instituto-geofisico-del-peru-en-el-2019

[5] Seismic Velocity Structure in the Area of the 2007, Mw 8.0, Pisco-Peru Earthquake: Implications for the Mechanics of Subduction in the Vicinity of the Nazca Ridge, Instituto Geofísico del Perú, 2020. [Online]. Available: https://www.gob.pe/institucion/igp/informes-publicaciones/1336290-seismic-velocity-structure-in-the-area-of-the-2007-mw-8-0-pisco-peru-earthquake-implications-for-the-mechanics-of-subduction-in-the-vicinity-of-the-nazca-ridge

[6] I. Bernal, and H. Tavera, "Seismic Velocity Structure in the Area of the 2007, Mw 8.0, Pisco-Peru Earthquake: Implications for the Mechanics of Subduction in the Vicinity of the Nazca Ridge," *International Journal of Geophysics*, vol. 2020, no. 1, 2020. [CrossRef] [Google Scholar] [Publisher Link]

[7] Ying Zhou, Mohammed Samier Sebaq, and Yi Xiao, "Energy Dissipation Demand and Distribution for Multi-Story Buildings with Fluid Viscous Dampers," *Engineering Structures*, vol. 253, 2022. [CrossRef] [Google Scholar] [Publisher Link]

[8] Munir Ahmed, "Fluid Viscous Dampers Locations in Reinforced-Concrete Core Wall Buildings," *Proceedings of the Institution of Civil Engineers - Structures and Buildings*, vol. 170, no. 1, pp. 33-50, 2017. [CrossRef] [Google Scholar] [Publisher Link]

[9] Vin Nguyen-Thai et al., "An Effective Optimum Design for Passive Viscous Damping Control Using FVDs/VWDs in Multi-Story Buildings," *Structures*, vol. 67, 2024. [CrossRef] [Google Scholar] [Publisher Link]

[10] A. Dilsiz et al., "Seismic Design and Performance of Reinforced Concrete Special Moment Resisting Frames with Wall Dampers," *Journal of Earthquake Engineering*, vol. 26, no. 2, pp. 744-763, 2022. [CrossRef] [Google Scholar] [Publisher Link]

[11] Abdullah Dilsiz, and Ali Ruzi Özuygur, "Suppression of the Torsional Irregularity of High-Rise Buildings Using Viscous Wall Dampers," *Bulletin of Earthquake Engineering*, vol. 20, pp. 4237-4257, 2022. [CrossRef] [Google Scholar] [Publisher Link]

[12] Norma E.030 Diseño Sismorresistente, pp. 1-81, 2020. [Online]. Available: https://drive.google.com/file/d/1W14N6JldWPN8wUZSqWZnUphg6C559bi-/view?usp=embed_facebook

[13] Google Maps, 2025. [Online]. Available: https://www.google.com/maps/@-12.0232057,-75.2320512,14z?entry=ttu&g_ep=EgoyMDI1MDcyMi4wIKXMDSoASAFQAw%3D%3D

[14] Angel Leandro Ccahua-Laqui et al., "Dominant Frequencies of the Site in Lima, Peru, by h/v Spectral Ratio of Seismic Records," *TECNIA*, vol. 32, no. 2, pp. 171-184, 2022. [CrossRef] [Google Scholar] [Publisher Link]

[15] Jaime Santos-Reyes, "How Useful are Earthquake Early Warnings? The Case of the 2017 Earthquakes in Mexico City," *International Journal of Disaster Risk Reduction*, vol. 40, 2019. [CrossRef] [Google Scholar] [Publisher Link]

[16] Edgar Tapia-Hernández, Mehmet Cemal Geneş, and Héctor Guerrero-Bobadilla, "Structural Behavior of Hospitals during the Kahramanmaraş Earthquake of February 6, 2023," *Earthquake Spectra*, vol. 41, no. 2, pp. 1589-1615, 2025. [CrossRef] [Google Scholar] [Publisher Link]

[17] Engineers Explain Why so Many Buildings Collapsed in Türkiye, Dynatec, 2023. [Online]. Available: https://dynatec.es/2023/02/16/los-ingenieros-explican-por-que-se-derrumbaron-tantos-edificios-en-turquia/?lang=en
[18] Ying Zhou et al., "A New Analytical Model for Viscous Wall Dampers and its Experimental Validation," *Engineering Structures*, vol. 163, pp. 224-240, 2018. [CrossRef] [Google Scholar] [Publisher Link]
[19] M.S. Mohammed et al., "Enhancing Seismic Performance of Buildings Using Viscous Wall Dampers," *2019 Pacific Conference on Earthquake Engineering and Annual NZSEE Conference*, pp. 1-8, 2019. [Google Scholar] [Publisher Link]
[20] Ali Erdem Çerçevik, Özgür Avşar, and Abdullah Dilsiz, "Optimal Placement of Viscous Wall Dampers in RC Moment Resisting Frames Using Metaheuristic Search Methods," *Engineering Structures*, vol. 249, 2021. [CrossRef] [Google Scholar] [Publisher Link]
[21] Navid Salami Pargoo, Farzad Hejazi, and Sarah Jabbar, "Preventing Seismic Pounding of Adjacent Structures Using Viscous Wall Damper Device," *Lecture Notes in Civil Engineering*, vol. 9, pp. 561-577, 2018. [CrossRef] [Google Scholar] [Publisher Link]
[22] A. Dilsiz et al., "Evaluation of Wall Damper Effectiveness on the Seismic Performance of Buildings," *Eleventh U.S. National Conference on Earthquake Engineering*, Los Angeles, California, pp. 1-11, 2019. [Google Scholar]
[23] M.A. Wasey, Muhammed Masihuddin Siddiqui, and M.A. Azeem, "Optimum Seismic Control Systems for Vertically Irregular Buildings," *Materials Today: Proceedings*, vol. 65, pp. 1674-1689, 2022. [CrossRef] [Google Scholar] [Publisher Link]
[24] Batchu Ramanjaneyulu et al., "Seismic Analysis of Vertically Irregular RCC High-Rise Buildings: A Study with Provision of FVD at Various Locations," *IOP Conference Series: Earth and Environmental Science, Third International Conference on Advances in Concrete and Construction Engineering for Sustainability*, Hyderabad, India, vol. 1409, no. 1, pp. 1-18, 2024. [CrossRef] [Google Scholar] [Publisher Link]
[25] Yanhui Liu, Jinbiao Wu, and Marco Donà, "Effectiveness of Fluid-Viscous Dampers for Improved Seismic Performance of Inter-Storey Isolated Buildings," *Engineering Structures*, vol. 169, pp. 276-292, 2018. [CrossRef] [Google Scholar] [Publisher Link]
[26] Romel Moises Olivera Perez et al., "Influence of Vertical Geometric Irregularity on the Seismic Response of High-Rise Buildings Equipped with Base Isolation System," *Civil Engineering and Architecture*, vol. 12, no. 3A, pp. 2091-2115, 2024. [CrossRef] [Google Scholar] [Publisher Link]
[27] M. Ahmed, N. Ahmed, and N. Haque, "Effective Placement of Fluid Viscous Damper in Irregular Shaped Reinforced Concrete Buildings," *Journal of Engineering Research, Innovation and Education*, vol. 4, no. 1, pp. 5-10, 2022. [Google Scholar]
[28] Magdalini Titirla, and Walid Larbi, "Comparative Analysis of Seismic Performance Enhancement in Irregular RC Buildings Using Friction and Viscous Dampers," *Procedia Structural Integrity*, vol. 64, pp. 968-974, 2024. [CrossRef] [Google Scholar] [Publisher Link]
[29] Momen Mohamed. M. Ahmed, Mohamed Abdel-Basset Abdo, and Waleed Abo El-Wafa Mohamed, "Vertical Geometric Irregularity Effect on Performance-Based Seismic Design for Moderate Rise RC Moment Resisting Frame Buildings," *Arabian Journal for Science and Engineering*, vol. 47, pp. 12333-12348, 2022. [CrossRef] [Google Scholar] [Publisher Link]
[30] H.M.S.C. Rathnasiri, J.A.S.C. Jayasinghe, and C.S. Bandara, "Development of Irregularity Index Based on Dynamic Characteristics to Quantify the Vertical Geometric Irregularities," *Engineer: Journal of the Institution of Engineers, Sri Lanka*, vol. 53, no. 1, pp. 41-51, 2020. [CrossRef] [Google Scholar] [Publisher Link]
[31] Comments on Standard E.030 Earthquake Resistant Design, Sencico, 2020. [Online]. Available: https://drive.google.com/file/d/1GlDLvL2OQCHLWNyRUBtoAHC4GhV0Z1Vg/view
[32] Pooya Zakian, and Ali Kaveh, "Seismic Design Optimization of Engineering Structures: A Comprehensive Review," *Acta Mechanica*, vol. 234, pp. 1305-1330, 2023. [CrossRef] [Google Scholar] [Publisher Link]
[33] Joshy Nichelson Castillo Curasma et al., "Structural Behavior of Building with First Level Height Variation Controlled by Viscous Fluid Damper," *Civil Engineering and Architecture*, vol. 13, no. 1, pp. 55-94, 2025. [CrossRef] [Google Scholar] [Publisher Link]
[34] S. Javadinasab Hormozabad, and S.M. Zahrai, "Innovative Adaptive Viscous Damper to Improve Seismic Control of Structures," *Journal of Vibration and Control*, vol. 25, no. 12, pp. 1833-1851, 2019. [CrossRef] [Google Scholar] [Publisher Link]
[35] Soheil Nikpour, Farzad Hejazi, and Mohd Saleh Jaafar, "Development of a Divergent Fluid Wall Damper for Framed Structures Subjected to Dynamic Loads," *Structural Control and Health Monitoring*, vol. 25, no. 3, 2018. [CrossRef] [Google Scholar] [Publisher Link]
[36] Viscous Wall Dampers Guidelines for Modeling, Dynamic Isolation Systems, 2025. [Online]. Available: https://www.dis-inc.com/pdf_files/VWD%20Model%20Guide%20Web%20May%2018.pdf
[37] Effy Hidayaty et al., "Numerical Analysis of Viscous Wall Dampers on Steel Frame," *MATEC Web of Conferences*, vol. 147, 2018. [CrossRef] [Google Scholar] [Publisher Link]
[38] Panagiota Katsimpini, "On the Seismic Response of Composite Structures Equipped with Wall Dampers under Multiple Earthquakes," *Modelling*, vol. 6, no. 1, pp. 1-21, 2025. [CrossRef] [Google Scholar] [Publisher Link]
[39] Fk. Lawmzela, and Gagandeep Singh, "Seismic Analysis of Irregular High-Rise Structures: Comparative Study on the Effectiveness of Fluid Viscous Dampers and Lead Rubber Bearing Systems," *AIP Conference Proceedings*, vol. 3305, no. 1, 2025. [CrossRef] [Google Scholar] [Publisher Link]